Annu. Rev. Nucl. Part. Sci. 1999. 49:163–216

PARTICLE PHYSICS FROM STARS

Georg G. Raffelt
Max-Planck-Institut für Physik (Werner-Heisenberg-Institut), Föhringer Ring 6, 80805 München, Germany; e-mail: raffelt@mppmu.mpg.de

Key Words astroparticle physics, stellar evolution, neutrinos, axions

■ **Abstract** Low-mass particles, such as neutrinos, axions, other Nambu-Goldstone bosons, and gravitons, are produced in the hot and dense interior of stars. Therefore, astrophysical arguments constrain the properties of these particles in ways that are often complementary to cosmological arguments and to laboratory experiments. This review provides an update on the most important stellar-evolution limits and discusses them in the context of other information from cosmology and laboratory experiments.

CONTENTS

0163-8998/99/1201-0163$08.00

1. INTRODUCTION

Astrophysical and cosmological arguments and observations have become part of the mainstream methodology to obtain empirical information on existing or hypothetical elementary particles and their interactions. The "heavenly laboratories" are complementary to accelerator and nonaccelerator experiments, notably at the "low-energy frontier" of particle physics, which includes the physics of neutrinos and other weakly interacting low-mass particles such as the hypothetical axions, novel long-range forces, and so forth.

The present review is dedicated to stars as particle-physics laboratories, or, more precisely, to what can be learned about weakly interacting low-mass particles from the observed properties of stars. The prime argument is that a hot and dense stellar plasma emits low-mass weakly interacting particles in great abundance. They subsequently escape from the stellar interior directly, without further interactions, and thus provide a local energy sink for the stellar medium. The astronomically observable impact of this phenomenon provides some of the most powerful limits on the properties of neutrinos, axions, and the like.

Once the particles have escaped, they can decay on their long way to Earth, allowing one to derive interesting limits on radiative decay channels from the absence of unexpected X-ray or γ-ray fluxes from the Sun or other stars.

Finally, the weakly interacting particles—thus far only the neutrinos from the Sun and supernova (SN) 1987A—can be directly detected at Earth, revealing important information on their properties.

The material covered here was reviewed in 1990, with a focus on axion limits, by Turner (1) and by Raffelt (2), and a very brief "Mini-Review" was included in the 1998 edition of the *Review of Particle Physics* (3). My 1996 book *Stars as Laboratories for Fundamental Physics* (4) treats these topics in much greater detail than is possible here. The present chapter is intended as a compact, up-to-date, and easily accessible source for the most important results and methods.

The subject of particle physics from stars is broader than both my expertise and the space available here. This chapter does not touch on the solar neutrino problem and its oscillation interpretation—this is a topic unto itself and has been extensively reviewed by other authors (e.g. 5–7). It is reviewed in this volume by Kayser et al (7a).

The high densities encountered in neutron stars make them ideal for studies and speculations concerning novel phases of nuclear matter (e.g. meson condensates or quark matter), an area covered by two recent books (8, 9). Quark stars are also the subject of an older review (10) and are covered in the proceedings of two topical conferences (11, 12).

Certain grand unified theories predict the existence of primordial magnetic monopoles. They would get trapped in stars and then catalyze the decay of nucleons by the Rubakov-Callan effect. The ensuing anomalous energy release is constrained by the properties of stars, in particular neutron stars and white dwarfs, a topic that was reviewed a long time ago (13). It was reexamined, and the limits were improved, in the wake of the discovery of the faintest white dwarf ever detected, which puts restrictive limits on an anomalous internal heat source (14).

Weakly interacting massive particles (WIMPs), notably in the guise of the supersymmetric neutralinos, are prime candidates for the cosmic dark matter. Some of them would get trapped in stars, annihilate with each other, and produce a secondary flux of high-energy neutrinos. The search for such fluxes from the Sun and the center of the Earth by present-day and future neutrino telescopes is the "indirect method" to detect galactic particle dark matter, an approach that is competitive with direct laboratory searches (see 15 for a review).

In this chapter, Sections 2–4 are devoted to a discussion of the main stellar objects that have been used to constrain low-mass particles, viz. the Sun, globular-cluster stars, compact stars, and SN 1987A. In Sections 5–7, the main constraints on neutrinos, axions, and novel long-range forces are summarized. Section 8 is given over to brief concluding remarks.

2. THE SUN

2.1 Basic Energy-Loss Argument

The Sun is the best-known star and is thus a natural starting point for our survey of astrophysical particle laboratories. It is powered by hydrogen burning, which amounts to the net reaction $4p + 2e^- \rightarrow {}^4\mathrm{He} + 2\nu_e + 26.73$ MeV, giving rise to a measured ν_e flux that now provides one of the most convincing indications for neutrino oscillations (5–7). Instead of neutrinos from nuclear processes, I focus here on particle fluxes that are produced in thermal plasma reactions. The photoneutrino process $\gamma + e^- \rightarrow e^- + \nu\bar{\nu}$ is a case in point, as is the production of gravitons from electron bremsstrahlung. The solar energy loss from such standard processes is small, but it may be large for hypothetical particles. To be specific, I consider axions (Section 6), which arise in a variety of reactions, and in particular by the Primakoff process in which thermal photons mutate into axions in the electric field of the medium's charged particles (Figure 1). In Section 6.2.1, I discuss direct search experiments for solar axions, whereas here I focus on the main topic of this review, the backreaction of a new energy loss on stars.

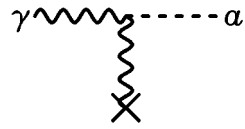

Figure 1 Primakoff production of axions in the Sun.

The Sun is a normal star that supports itself against gravity by thermal pressure, as opposed to degenerate stars such as white dwarfs, which are supported by electron degeneracy pressure. If one pictures the Sun as a self-gravitating monatomic gas in hydrostatic equilibrium, the "atoms" obey the virial theorem $\langle E_{\rm kin}\rangle = -\frac{1}{2}\langle E_{\rm grav}\rangle$. The most important consequence of this relationship is that extracting energy from such a system, i.e. reducing the total energy $\langle E_{\rm kin}\rangle + \langle E_{\rm grav}\rangle$, leads to contraction and to an *increase* of $\langle E_{\rm kin}\rangle$. Therefore, all else being equal, axion losses lead to contraction and heating. The nuclear energy generation rate scales with a high power of the temperature. Therefore, the heating implied by the new energy loss causes increased nuclear burning—the star finds a new equilibrium configuration where the new losses are compensated by an increased rate of energy generation.

The main lesson is that the new energy loss does not "cool" the star; it leads to heating and an increased consumption of nuclear fuel. The Sun, where energy is transported from the central nuclear furnace by radiation, actually overcompensates the losses and brightens, whereas it would dim if the energy transfer were by convection. Either behavior is understood by a powerful "homology argument," in which the nonlinear interplay of the equations of stellar structure is represented in a simple analytic fashion (16).

The solar luminosity is well measured, yet this brightening effect is not observable because all else need not be equal. The present-day luminosity of the Sun depends on its unknown initial helium mass fraction Y; in a solar model, Y has to be adjusted such that $L_\odot = 3.85 \times 10^{33}$ erg s^{-1} is reproduced after 4.6×10^9 years of nuclear burning. For solar models with axion losses, the required presolar helium abundance Y as a function of the axion-photon coupling constant $g_{a\gamma}$ is shown in Table 1. The axion luminosity L_a is also given, as well as the central helium abundance Y_c, density ρ_c, and temperature T_c of the present-day Sun.

Even axion losses as large as $L_\odot$ can be accommodated by reducing the presolar helium mass fraction from about 27% to something like 23% (17, 18). The "standard Sun" has completed about half of its hydrogen-burning phase. Therefore, the anomalous energy losses cannot exceed approximately $L_\odot$ or else the Sun could not have reached its observed age. Indeed, for $g_{10} = 30$, no consistent present-day Sun could be constructed for any value of Y (18). The emission rate of other hypothetical particles would have a different temperature and density dependence from the Primakoff process, yet the general conclusion remains the same—that a novel energy loss must not exceed approximately $L_\odot$.

TABLE 1 Solar-model parameters and relative detection rates in the Cl, Ga, and water neutrino observatories as a function of the axion-photon coupling constant $g_{10} \equiv g_{a\gamma}/(10^{-10}\ \mathrm{GeV}^{-1})$ according to Reference 17

g_{10}	L_a [$L_\odot$]	Y	Y_c	ρ_c [g cm^{-3}]	T_c [10^7 K]	Cl	Ga	H_2O
0	0	0.266	0.633	153.8	1.563	1	1	1
4.5	0.04	0.265	0.641	158.0	1.575	1.07	1.16	1.20
10	0.20	0.257	0.679	177.5	1.626	1.45	2.2	2.4
15	0.53	0.245	0.751	218.3	1.722	2.5	6.0	6.7
20	1.21	0.228	0.914	324.2	1.931	6.4	20	23

2.2 Solar Neutrino Measurements

This crude limit is improved by the solar neutrino flux, which has been measured in five different observatories with three different spectral response characteristics, i.e. by the absorption on chlorine, gallium, and by the water Cherenkov technique. The axionic solar models produce larger neutrino fluxes; Table 1 shows the expected detection rates for the Cl, Ga, and H_2O experiments relative to the standard case. For $g_{10} \lesssim 10$, one can still find oscillation solutions to the observed ν_e deficit, but larger energy-loss rates appear to be excluded (17).

Once the neutrino oscillation hypothesis has been more firmly established and the mixing parameters are better known, the neutrino measurements may be used to pin down the central solar temperature, allowing one to constrain novel energy losses with greater precision. For now, it appears safe to conclude that the Sun does not emit more than a few tenths of $L_\odot$ in new forms of radiation.

2.3 Helioseismology

Over the past few years, the precision measurements of the solar p-mode frequencies have provided a more reliable way to study the solar interior. For example, the convective surface layer is found to reach down to 0.710–0.716 $R_\odot$ (19), the helium content of these layers to exceed 0.238 (20). Gravitational settling has reduced the surface helium abundance by about 0.03, so that the presolar value must have been at least 0.268, in good agreement with standard solar models. The reduced helium content required of the axionic solar models in Table 1 disagrees significantly with this lower limit for $g_{10} \geq 10$.

One may also invert the p-mode measurements to construct a "seismic model" of the solar sound-speed profile (e.g. 21). All modern standard solar models agree well with the seismic model within its uncertainties (Figure 2, shaded band), which mostly derive from the inversion method itself, not from the measurements. Figure 2 also shows the difference between the sound-speed profile of a standard solar model and those including axion losses. For $g_{10} \geq 10$, the difference is larger

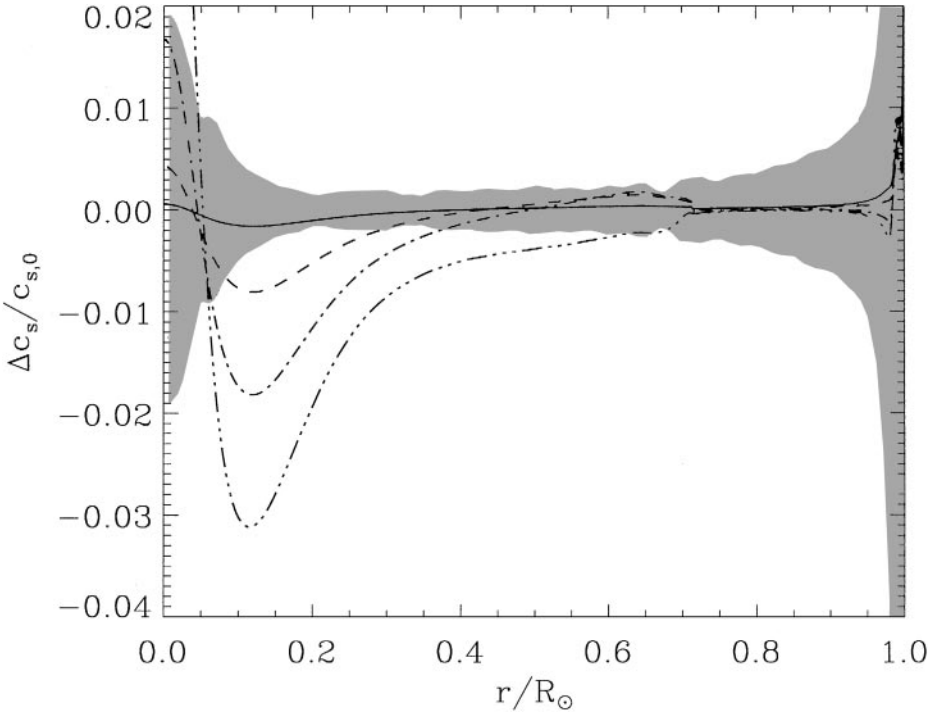

Figure 2 Fractional difference in sound-speed profiles of solar models with axion losses compared with the reference model (17). The shaded area is the uncertainty of the seismic model (20). The axion-photon coupling constant was $g_{10} = 4.5$ (solid line), 10 (short-dashed line), 15 (dash-dotted line), 20 (dash-triple-dotted line).

than the uncertainties of the seismic model, implying a limit

$$g_{a\gamma} \lesssim 10 \times 10^{-10}\ \mathrm{GeV}^{-1}. \qquad 1.$$

Other cases may be different in detail, but it appears safe to assume that any new energy-loss channel must not exceed something like 10% of $L_\odot$.

2.4 "Strongly" Interacting Particles

Thus far, we have assumed that the new particles couple so weakly that they escape from the stellar interior without further interactions, in analogy to neutrinos or gravitons. They emerge from the entire stellar volume, i.e. their emission amounts to a local energy sink for the stellar plasma. But what if the particles interact so strongly that their mean free path is less than the solar radius?

The impact of such particles on a star is comparable to that of photons, which are also "trapped" by their "strong" interaction. Their continuous thermal production and reabsorption amounts to the net transfer of energy from regions of higher

temperature to cooler regions. In the Sun, this radiative form of energy transfer is more important than conduction by electrons or convection, except in the outer layers. A particle that interacts more weakly than photons is more effective because it travels a larger distance before reabsorption—the ability to transfer energy is proportional to the mean free path. The properties of the Sun roughly confirm the standard photon opacities, so that a new particle would have to interact more strongly than photons to be allowed (22, 23).

Therefore, contrary to what is sometimes stated in the literature, a new particle is by no means allowed just because its mean free path is less than the stellar dimensions. The impact of a new particle is maximal when its mean free path is of the order of the stellar radius. Of course, one is usually interested in very weakly interacting particles, so that this point is moot.

3. LIMITS ON STELLAR ENERGY LOSSES

3.1 Globular-Cluster Stars

3.1.1 Evolution of Low-Mass Stars The discussion in the previous section suggests that the emission of new weakly interacting particles from stars primarily modifies the time scale of evolution. For the Sun, this effect is less useful to constrain particle emission than, say, the modified p-mode frequencies or the direct measurement of the neutrino fluxes. However, the observed properties of other stars provide far more restrictive limits on their evolutionary time scales, so that anomalous modes of energy loss can be far more tightly constrained. I begin with globular-cluster stars, which, along with SN 1987A, are the most successful example of astronomical observations that provide nontrivial limits on the properties of elementary particles.

Our galaxy has about 150 globular clusters, such as M3 (Figure 3), which are gravitationally bound systems of up to a million stars. In Figure 4, the stars of the cluster M3 are arranged according to their color or surface temperature (horizontal axis) and brightness (vertical axis) in the usual way, leading to a characteristic pattern that allows rather precise tests of the theory of stellar evolution, and notably allows quantitative measurements of certain evolutionary time scales. Globular clusters are the oldest objects in the galaxy and thus are almost as old as the universe. The stars in a given cluster all formed at about the same time with essentially the same chemical composition, differing primarily in their mass. Because more massive stars evolve faster, present-day globular-cluster stars are somewhat below $1\,\mathcal{M}_\odot$,[1] so that we are concerned with low-mass stars ($\mathcal{M} \lesssim 2\,\mathcal{M}_\odot$). (See 26, 27 for textbook expositions of stellar structure and evolution.)

[1]The letter $\mathcal{M}$ denotes stellar masses with $1\,\mathcal{M}_\odot = 2 \times 10^{33}$ g the solar mass. The letter M is traditionally reserved for the absolute stellar brightness (in magnitudes or mag). The total or bolometric brightness is defined as $M_{\rm bol} = 4.74 - 2.5\log_{10}(L/L_\odot)$, with the solar luminosity $L_\odot = 3.85 \times 10^{33}$ erg s^{-1}.

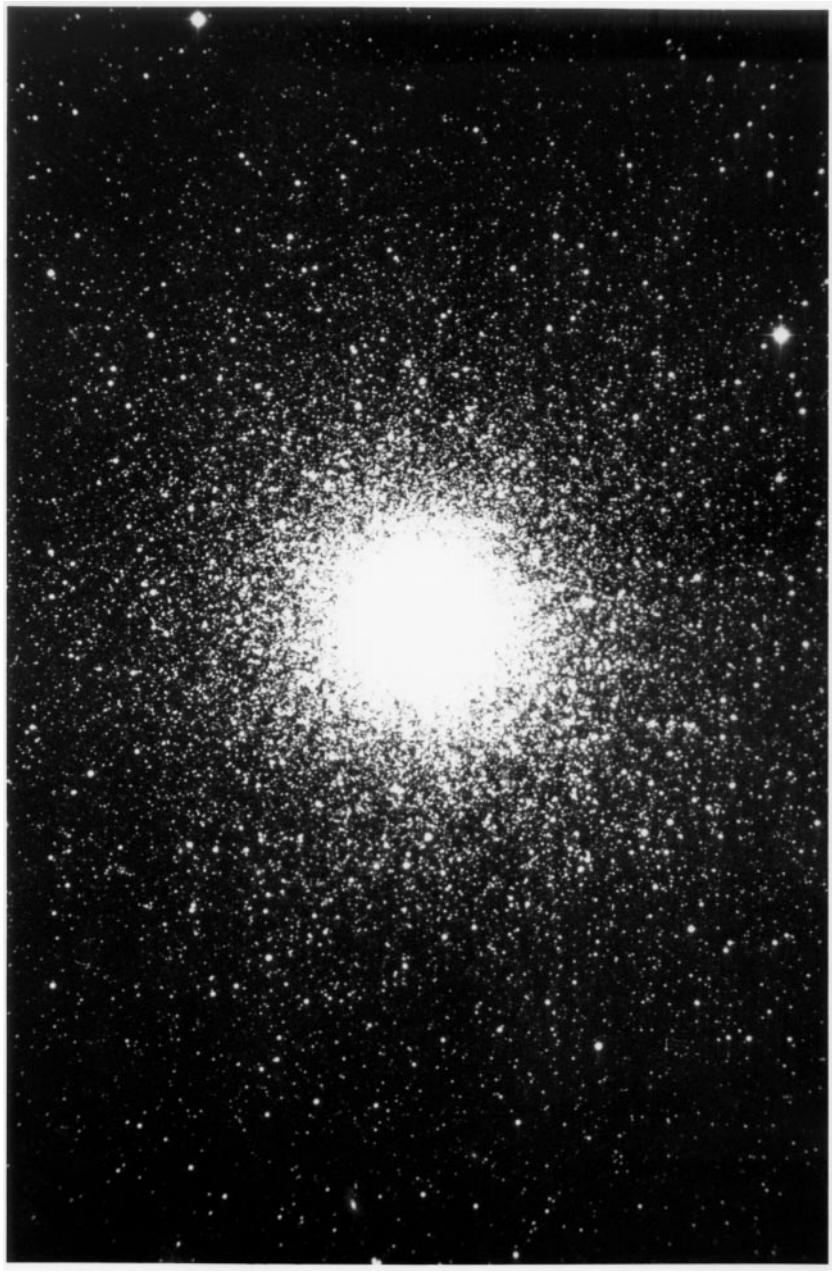

Figure 3 Globular cluster M3. (Image courtesy of Palomar/Caltech.)

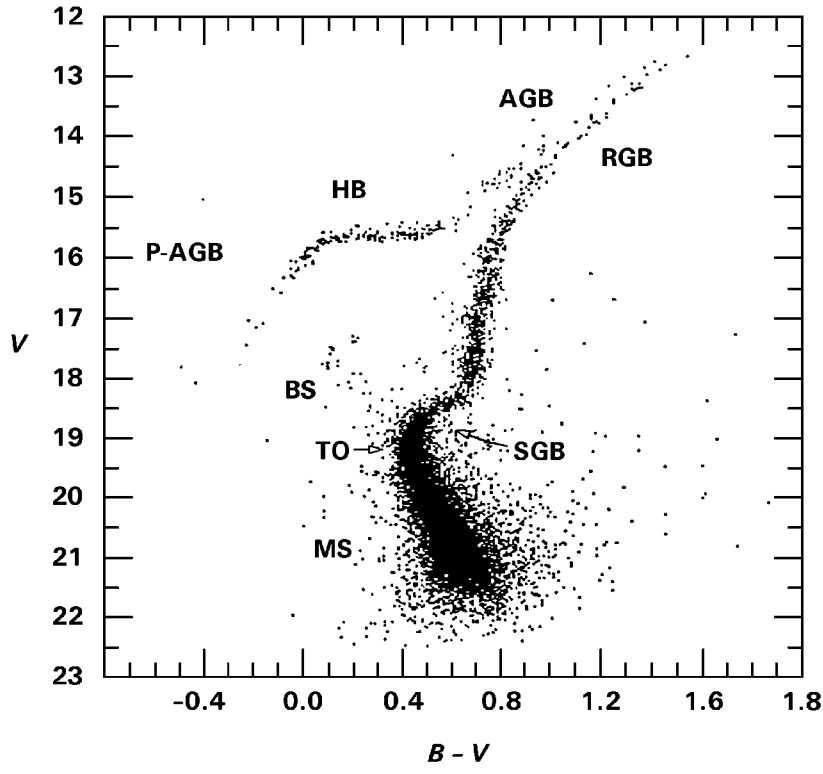

Figure 4 Color-magnitude diagram for the globular cluster M3, based on the photometric data of 10,637 stars (24). Vertical axis shows the brightness in the visual (V) band; horizontal axis shows the difference between B (blue) and V brightness, i.e. a measure of the color and thus surface temperature, where blue (hot) stars lie toward the left. The classification for the evolutionary phases is as follows (25). MS (main sequence): core hydrogen burning. BS, blue stragglers. TO (main-sequence turnoff): central hydrogen is exhausted. SGB (subgiant branch): hydrogen burning in a thick shell. RGB (red-giant branch): hydrogen burning in a thin shell with a growing core until helium ignites. HB (horizontal branch): helium burning in the core and hydrogen burning in a shell. AGB (asymptotic giant branch): helium and hydrogen shell burning. P-AGB (post-asymptotic giant branch): final evolution from the AGB to the white-dwarf stage.

A star begins its life on the main sequence (MS), where it burns hydrogen in its center. Different locations on the MS in a color-magnitude diagram (Figure 4) correspond to different masses; more massive stars shine more brightly. When central hydrogen is exhausted, the star develops a degenerate helium core, with hydrogen burning in a shell. Curiously, the stellar envelope expands, leading to a large surface area and thus a low surface temperature (red color)—the star becomes a “red giant.” The luminosity is governed by the gravitational potential at the edge

of the growing helium core, so that these stars become ever brighter—they ascend the red-giant branch (RGB). The higher a star is on the RGB, the more massive and compact its helium core.

The core grows until about $0.5\,\mathcal{M}_\odot$, when it has become dense and hot enough to ignite helium. The ensuing core expansion reduces the gravitational potential at its edge and thus lowers the energy production rate in the hydrogen shell source, dimming the star. Helium ignites at a fixed core mass, but the envelope mass differs due to varying rates of mass loss on the RGB, leading to different surface areas and thus different surface temperatures. These stars therefore occupy the horizontal branch (HB) in the color-magnitude diagram. In Figure 4, the HB turns down on the left (blue color), where much of the luminosity falls outside the V filter; in terms of the total or "bolometric" brightness, the HB is truly horizontal.

Finally, when helium is exhausted, a degenerate carbon-oxygen core develops, leading to a second ascent on what is called the asymptotic giant branch (AGB). These low-mass stars cannot ignite their carbon-oxygen cores; they become white dwarfs after shedding most of their envelope.

The advanced evolutionary phases are fast compared with the MS duration, which is about 10^{10} yr for stars somewhat below $1\,\mathcal{M}_\odot$. For example, the ascent on the upper RGB and the HB phase each take around 10^8 yr. Therefore, the distribution of stars along the RGB and beyond can be taken as an "isochrone" for the evolution of a single star, i.e. a time series of snapshots for the evolution of a single star with a fixed initial mass. Put another way, the number distributions of stars along the different branches are a direct measure for the duration of the advanced evolutionary phases. The distribution along the MS is different in that it measures the distribution of initial masses.

3.1.2 Core Mass at Helium Ignition Anomalous energy losses modify this picture in measurable ways. I first consider an energy-loss mechanism that is more effective in the degenerate core of a red giant before helium ignition than on the HB, so that the post-RGB evolution is standard. Because an RGB star's helium core is supported by degeneracy pressure, there is no feedback between energy loss and pressure—the core is actually cooled. Helium burning ($3^4\mathrm{He} \rightarrow {}^{12}\mathrm{C}$) depends very sensitively on temperature and density, so that the cooling delays the ignition of helium, leading to a larger core mass $\mathcal{M}_c$. This process has several observable consequences.

First, the brightness of a red giant depends on its core mass, so that the RGB would extend to larger luminosities, causing an increased brightness difference $\Delta M_{\rm HB}^{\rm tip}$ between the HB and the RGB tip. Second, an increased $\mathcal{M}_c$ implies an increased helium-burning core on the HB. For a certain range of colors, these stars are pulsationally unstable and are called RR Lyrae stars. From the measured RR Lyrae luminosity and pulsation period, one can infer $\mathcal{M}_c$ on the basis of their so-called mass-to-light ratio A. Third, the increased $\mathcal{M}_c$ increases the luminosity of RR Lyrae stars, so that absolute determinations of their brightness $M_{\rm RR}$ allow

one to constrain the range of possible core masses. Fourth, the number ratio R of HB stars vs RGB stars brighter than the HB is modified.

These observables also depend on the measured cluster metallicity, as well as the unknown helium content, which is usually expressed in terms of $Y_{\rm env}$, the envelope helium mass fraction. Because globular clusters formed shortly after the big bang, their initial helium content must be close to the primordial value of 22–25%. $Y_{\rm env}$ should be close to this number because the initial mass fraction is somewhat depleted by gravitational settling and is somewhat increased by convective dredge-up of processed, helium-rich material from the inner parts of the star.

An estimate of $\mathcal{M}_c$ from a global analysis of these observables, except A, was performed (28) and reanalyzed (4). A was used in Reference 29 and in an independent analysis using all four observables (30). Figure 5 shows the allowed core-mass excess $\delta\mathcal{M}_c$ and envelope helium mass fraction $Y_{\rm env}$ from the analyses (4, 30; references to the original observations are found in these papers).

Figure 5 suggests that, within the given uncertainties, the different observations overlap at the standard core mass ($\delta\mathcal{M}_c = 0$) and at an envelope helium mass fraction $Y_{\rm env}$ that is compatible with the primordial helium abundance. Of course, the error bands do not have a simple interpretation because they combine observational and estimated systematic errors, which involve some subjective judgment by the authors. The difference between the two panels of Figure 5 indicates how sensitive the conclusions are to these more arbitrary aspects of the analysis. As a nominal limit, it appears safe to adopt $|\delta\mathcal{M}_c| \lesssim 0.025$ or $|\delta\mathcal{M}_c|/\mathcal{M}_c \lesssim 5\%$; how much additional "safety margin" to include is a somewhat arbitrary decision that is difficult to make objective in the sense of a statistical confidence level.

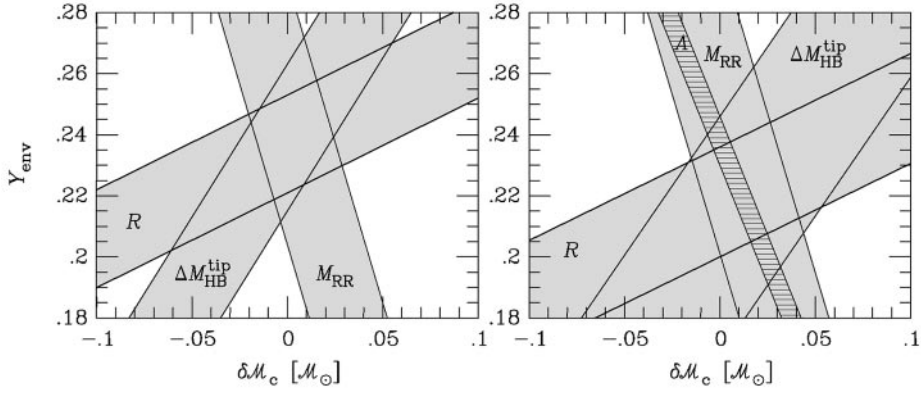

Figure 5 Allowed values for a core-mass excess at helium ignition $\delta\mathcal{M}_c$ and the envelope helium mass fraction $Y_{\rm env}$ of evolved globular-cluster stars. (Left after Reference 4, right after Reference 30.) The observables are the brightness difference $\Delta M_{\rm HB}^{\rm tip}$ between the HB and the RGB tip, the RR Lyrae mass-to-light ratio A, their absolute brightness $M_{\rm RR}$, and the number ratio R between HB and RGB stars.

This limit can be translated into an approximate limit on the average anomalous energy-loss rate ϵ_x of a helium plasma (4),

$$\epsilon_x \lesssim 10 \text{ erg g}^{-1} \text{ s}^{-1} \quad \text{at} \quad T \approx 10^8 \text{ K}, \quad \rho \approx 2 \times 10^5 \text{ g cm}^{-3}. \qquad 2.$$

The density represents the approximate average of a red-giant core before helium ignition; the value at its center is about 10^6 g cm^{-3}. The main standard-model neutrino emission process is plasmon decay $\gamma \to \nu\bar{\nu}$ with a core average of about 4 erg g^{-1} s^{-1}. Therefore, Equation 2 means that a new energy-loss channel must be less effective than a few times the standard neutrino losses.

3.1.3 Helium-Burning Lifetime of Horizontal-Branch Stars We now turn to an energy-loss mechanism that becomes effective in a nondegenerate medium. We imagine that the core expansion after helium ignition "switches on" an energy-loss channel that was negligible on the RGB. Therefore, the pre-HB evolution is taken to be standard. As in the case of the Sun (Section 2.1), there is little change in the HB stars' brightness; rather, they consume their nuclear fuel faster and thus begin to ascend the AGB sooner. The net observable effect is a reduction of the number of HB relative to RGB stars.

From the measured HB/RGB number ratios in 15 globular clusters (31), and with plausible assumptions about the uncertainties of other parameters, one concludes that the duration of helium burning agrees with stellar-evolution theory to within about 10% (4). This implies that the new energy loss of the helium core should not exceed about 10% of its standard energy production rate. Therefore, the new energy-loss rate at average core conditions is constrained by (4)

$$\epsilon_x \lesssim 10 \text{ erg g}^{-1} \text{ s}^{-1} \quad \text{at} \quad T \approx 0.7 \times 10^8 \text{ K}, \quad \rho \approx 0.6 \times 10^4 \text{ g cm}^{-3}. \qquad 3.$$

This limit is slightly more restrictive than the often-quoted "red-giant bound," corresponding to $\epsilon_x \lesssim 100$ erg g^{-1} s^{-1} at $T = 10^8$ K and $\rho = 10^4$ g cm^{-3}. It was based on the helium-burning lifetime of the "clump giants" in open clusters (32). They have fewer stars, leading to statistically less significant limits. The clump giants are the physical equivalent of HB stars, except that they occupy a common location at the base of the RGB, the "red-giant clump."

3.1.4 Applications After the energy-loss argument has been condensed into the simple criteria of Equations 2 and 3, it can be applied almost mechanically to a variety of cases. The main task is to identify the dominant emission process for the new particles and to calculate the energy-loss rate ϵ_x for a helium plasma at the conditions specified in Equations 2 or 3. The most important limits are discussed in the context of specific particle-physics hypotheses in Sections 5–7. These and similar arguments were used to constrain neutrino electromagnetic properties (28, 29, 32–37), axions (18, 38–52), paraphotons (53), the photoproduction cross section on ^{4}He of new bosons (54, 55), the Yukawa couplings of new bosons to baryons or electrons (56, 57), and supersymmetric particles (58–60).

It is also possible to calculate numerical evolution sequences, including new energy losses (18, 29, 35, 37, 52, 61). Comparing the results from such studies with what one finds from Equations 2 and 3 reveals that, in view of the overall theoretical and observational uncertainties, it is indeed enough to use these simple criteria (4).

3.2 White Dwarfs

White dwarfs are another case where astronomical observations provide useful limits on new stellar energy losses. These compact objects are the remnants of stars with initial masses of up to several $\mathcal{M}_\odot$ (27, 62). For low-mass progenitors, the evolution proceeds as described in Section 3.1.1. When they ascend the AGB they eventually shed most of their envelope mass. The degenerate carbon-oxygen core, having reached something like $0.6\,\mathcal{M}_\odot$, never ignites. Its subsequent evolution is simply one of cooling, dominated first by neutrino losses throughout its volume, later by surface photon emission.

The cooling speed can be observationally inferred from the "luminosity function," i.e. the white-dwarf number density per brightness interval. Because white dwarfs are intrinsically dim, they are observed only in the solar neighborhood, out to perhaps 100 pc (1 pc = 3.26 lyr), which is far less than the thickness of the galactic disk. The measured luminosity function (Figure 6) reveals that there are few bright white dwarfs and many faint ones. The dotted line represents Mestel's cooling law (62, 66), an analytic treatment based on surface photon cooling. The observed luminosity function dips at the bright end, a behavior ascribed to neutrino emission, which quickly "switches off" as the star cools.

The luminosity function drops sharply at the faint end. Even the oldest white dwarfs have not yet cooled any further, implying that they were born 8–12 Gyr ago, in good agreement with the estimated age of the galaxy. Therefore, a novel cooling agent cannot be much more effective than the surface photon emission. This conclusion also follows from the agreement between the implied birthrate and independent estimates. The shape of the luminosity function can be deformed for an appropriate temperature dependence of the particle emission rate, e.g. enhancing the "neutrino dip" at the bright end. Finally, white dwarfs in a certain range of surface temperatures are pulsationally unstable and are called ZZ Ceti stars. The pulsation period of a few minutes depends on the luminosity; the period decrease thus depends on the cooling speed. For G117–B15A, the period change was measured (67, 68), implying a somewhat large cooling rate. Although this discrepancy may be worrisome, these measurements should probably be taken as an approximate confirmation of the predicted white dwarf cooling speed.

White dwarfs were used to constrain the axion-electron coupling (69–74). It was also noted that the somewhat large period decrease of G117–B15A could be ascribed to axion cooling (75). Finally, a limit on the neutrino magnetic dipole moment was derived (73). Reference 4 provides a detailed review of these limits;

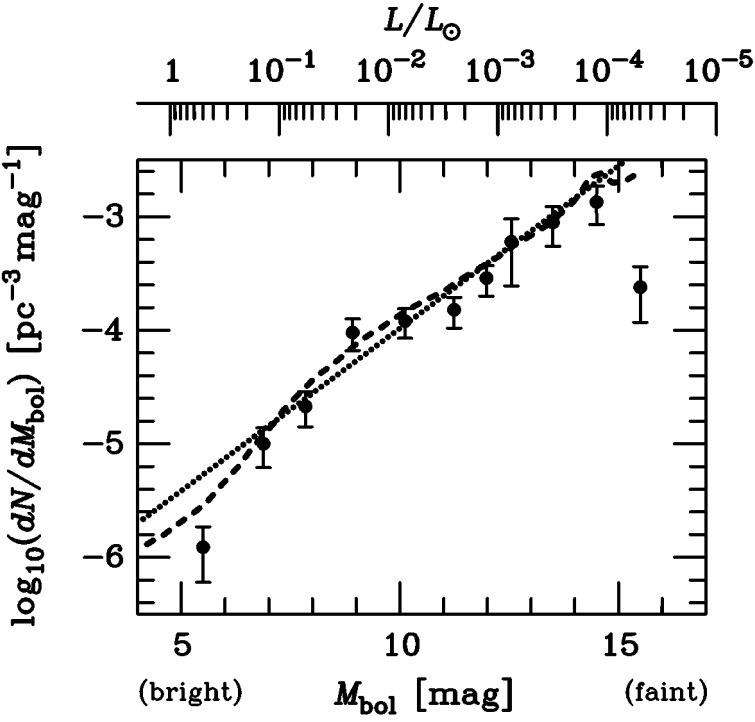

Figure 6 Observed white-dwarf luminosity function (63, 64). Dotted line, Mestel's cooling law with a constant birthrate of 10^{-3} pc^{-3} Gyr^{-1}. Dashed line, cooling curve of a $0.6\,\mathcal{M}_\odot$ white dwarf, which includes neutrino losses (65) assuming the same constant birthrate.

they are somewhat weaker than those from globular-cluster stars but are on the same general level. Therefore, white-dwarf cooling essentially corroborates some of the globular-cluster limits, but it does not improve on them.

3.3 Old Neutron Stars

Neutron stars are the compact remnants of stars with initial masses beyond about $8\,\mathcal{M}_\odot$. After their formation in a core-collapse supernova (Section 4), they evolve by cooling, which is accelerated by a new energy-loss channel. Neutron-star cooling can now be observed by satellite-borne X-ray measurements of the thermal surface emission of several old pulsars (see 76 for a recent review).

Limits on axions (77–79) and on neutrino magnetic dipole moments (80) have been derived. These bounds are much weaker than those from SN 1987A or globular clusters. Turning this around, anomalous cooling effects by particle emission are probably not important in old neutron stars, leaving them as laboratories for many of the other uncertain bits of input physics, such as the existence of new

phases of nuclear matter (8, 9, 76, 81, 82). If a neutron star converts into a strange-matter star, an axion burst emerges (83), but as yet this effect has not provided new empirical information on axion properties.

4. SUPERNOVAE

4.1 SN 1987A Neutrino Observations

When the explosion of the star Sanduleak −69 202 in the Large Magellanic Cloud, a satellite galaxy of our Milky Way at a distance of about 50 kpc (165,000 lyr), was detected on February 23, 1987, it became possible for the first time to measure the neutrino emission from a nascent neutron star, which made this supernova (SN 1987A) one of the most important stellar particle-physics laboratories (84–86).

A type II supernova explosion (87–92) is physically the implosion of an evolved massive star ($\mathcal{M} \gtrsim 8\,\mathcal{M}_\odot$) that has become an "onion-skin structure" with several burning shells surrounding a degenerate iron core. It cannot gain further energy by fusion, so it becomes unstable when it has reached the limiting mass (the Chandrasekhar mass) of 1–2 $\mathcal{M}_\odot$ that can be supported by electron-degeneracy pressure. The ensuing collapse is intercepted when the equation of state stiffens at around nuclear density (3×10^{14} g cm^{-3}), corresponding to a core size of a few tens of kilometers. At temperatures of tens of millions of electron volts, this compact object is opaque to neutrinos. The gravitational binding energy of the newborn neutron star ("proto–neutron star") of about 3×10^{53} erg is thus radiated over several seconds from the "neutrino sphere." Crudely put, the collapsed SN core cools by thermal neutrino emission from its surface.

The neutrino signal from SN 1987A (Figure 7) was observed by the $\bar{\nu}_e p \to n e^+$ reaction in several detectors (86). The number of events, their energies, and the distribution over several seconds corresponds well to theoretical expectations. Thus, these data have been interpreted as a confirmation of the standard picture—a compact remnant formed that emitted its energy by quasithermal neutrino emission. (See 96, 97 for detailed statistical analyses of the data.)

The signal does show a number of "anomalies." The average $\bar{\nu}_e$ energies inferred from the Irvine-Michigan-Brookhaven (IMB) and Kamiokande observations are quite different (98, 99). The large time gap of 7.3 s between the first eight and the last three Kamiokande events looks worrisome (100). The distribution of the final-state positrons from the $\bar{\nu}_e p \to n e^+$ capture reaction should be isotropic, but it is found to be significantly peaked away from the direction of the SN (55, 101, 102). In the absence of other explanations, these features have been blamed on statistical fluctuations in the sparse data.

4.2 Signal Dispersion

A dispersion of the neutrino burst can be caused by a time-of-flight delay from a nonvanishing neutrino mass (103). The arrival time from SN 1987A at a distance

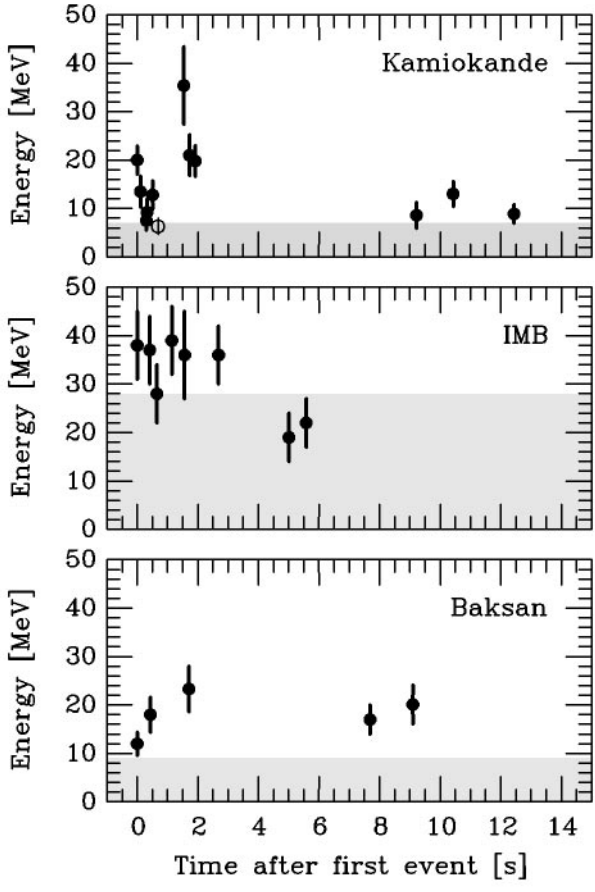

Figure 7 SN 1987A neutrino observations at Kamiokande (93), IMB (94), and Baksan (95). The energies refer to the secondary positrons from the reaction $\bar{\nu}_e p \rightarrow ne^+$. In the shaded area, the trigger efficiency is less than 30%. The clocks have unknown relative offsets; in each case, the first event was shifted to $t = 0$. In Kamiokande, the event marked as an open circle is attributed to background.

D would be delayed by

$$\Delta t = 2.57\ \mathrm{s}\left(\frac{D}{50\ \mathrm{kpc}}\right)\left(\frac{10\ \mathrm{MeV}}{E_\nu}\right)^2\left(\frac{m_\nu}{10\ \mathrm{eV}}\right)^2. \qquad 4.$$

Because the $\bar{\nu}_e$ were registered within a few seconds and had energies in the 10-MeV range, m_{ν_e} is limited to $\lesssim$10 eV. Detailed analyses reveal that the pulse duration is consistently explained by the intrinsic SN cooling time and that $m_{\nu_e} \lesssim 20$ eV is implied as something like a 95% CL limit (96, 104).

The apparent absence of a time-of-flight dispersion effect of the $\bar{\nu}_e$ burst was also used to constrain a "millicharge" of these particles (they would be deflected in the galactic magnetic field) (5, 105), a quantum field theory with a fundamental length scale (106), and deviations from the Lorentz rule of adding velocities (107). Limits on new long-range forces acting on the neutrinos (108–112) seem to be invalidated in the most interesting case of a long-range leptonic force by screening from the cosmic background neutrinos (113).

The SN 1987A observations confirm that the visual SN explosion occurs several hours after the core collapse and thus after the neutrino burst. Again, there is no apparent time-of-flight delay of the relative arrival times between the neutrino burst and the onset of the optical light curve, allowing confirmation of the equality of the relativistic limiting velocity for these particle types to within 2×10^{-9} (114, 115). Moreover, the Shapiro time delay in the gravitational field of the galaxy of neutrinos and photons agrees within about 4×10^{-3} (116), constraining certain alternative theories of gravity (117, 118).

4.3 Energy-Loss Argument

The late events in Kamiokande and IMB reveal that the signal duration was not anomalously short. Very weakly interacting particles would freely stream from the inner core, removing energy that otherwise would power the late-time neutrino signal. Therefore, its observed duration can be taken as evidence against such novel cooling effects. This argument has been advanced to constrain axion-nucleon couplings (119–127), majorons (128–134), supersymmetric particles (135–142), and graviton emission in quantum-gravity theories with higher dimensions (143, 144). It has also been used to constrain right-handed neutrinos interacting by a Dirac mass term (120, 145–155), mixed with active neutrinos (156, 157), interacting through right-handed currents (120, 158–161), a magnetic dipole moment (162–166), or an electric form factor (167, 168). Many of these results are reviewed in Sections 5–7 in the context of specific particle-physics hypotheses.

Here I illustrate the general argument with axions (Section 6) that are produced by nucleon bremsstrahlung $NN \to NNa$, so that the energy-loss rate depends on the axion-nucleon Yukawa coupling g_{aN}. Figure 8 shows the expected neutrino-signal duration as a function of g_{aN}. With increasing g_{aN}, corresponding to an increasing energy-loss rate, the signal duration drops sharply. For a sufficiently large g_{aN}, however, axions no longer escape freely; they are trapped and thermally emitted from the "axion sphere" at unit optical depth. Beyond some coupling strength, axions are less important than neutrinos and cannot be excluded.

However, particles on the "strong interaction" side of this argument need not be allowed. They could be important for the energy transfer during the infall phase, and they could produce events in the neutrino detectors. For example, "strongly coupled" axions in a large range of g_{aN} are actually excluded because they would have produced too many events by their absorption on ^{16}O (169).

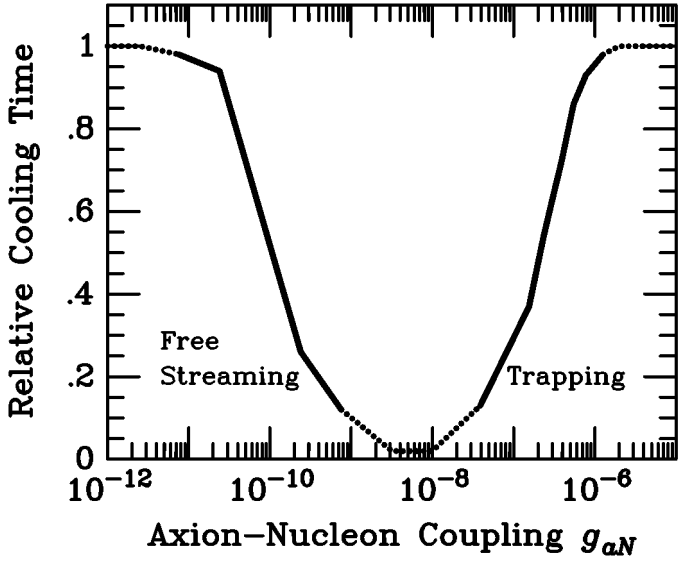

Figure 8 Relative duration of SN neutrino cooling as a function of the axion-nucleon coupling. Freely streaming axions are emitted from the entire core volume, trapped ones from the "axion sphere." The solid line follows from the numerical calculations (124, 125); the dotted line is an arbitrary continuation.

Likewise, particles on the free-streaming side can cause excess events in the neutrino detectors. For example, right-handed neutrinos escaping from the inner core could become "visible" by decaying into left-handed states (170) or by spin-precessing in the galactic magnetic field if they have a dipole moment.

Returning to the general argument, one can estimate a limit on the energy-loss rate on the free-streaming side by the simple criterion that the new channel should be less effective than the standard neutrino losses, corresponding to (4)

$$\epsilon_x \lesssim 10^{19}\ \mathrm{erg\ g^{-1}\ s^{-1}} \quad \text{at} \quad \rho = 3 \times 10^{14}\ \mathrm{g\ cm^{-3}}, \quad T = 30\ \mathrm{MeV}. \qquad 5.$$

The density is the core average, the temperature an average during the first few seconds. Some authors find higher temperatures, but for a conservative limit, it is preferable to stick to a value at the lower end of the plausible range. At these conditions, the nucleons are partially degenerate whereas the electrons are highly degenerate. Several detailed numerical studies reveal that this simple criterion corresponds to approximately halving the neutrino signal duration (4).

A simple analytic treatment is far more difficult on the trapping side (see 121 for an example in the context of axions).

The SN 1987A energy-loss argument tends to be most powerful at constraining new particle interactions with nucleons. Therefore, it is necessary to calculate the interaction rate with a hot and dense nuclear medium that is dominated by

many-body effects. Besides the sparse data, the theoretical treatment of the emission rate is the most problematic aspect of this method.

4.4 Radiative Neutrino Decays

If neutrinos have masses, one expects to find that the heavier neutrinos are unstable and decay radiatively as $\nu \to \nu'\gamma$. SN 1987A is thought to have emitted similar fluxes of neutrinos and antineutrinos of all flavors, so that one would have expected a burst of γ-rays in coincidence with the neutrinos. No excess counts were observed in the γ-ray spectrometer (GRS) on the solar maximum mission (SMM) satellite (171, 172), leading to restrictive limits on neutrino decays (171–175). The GRS happened to go into calibration mode about 223 s after the neutrino burst, but for low-mass neutrinos ($m_\nu \lesssim 40$ eV), the entire γ-ray burst would have been captured, leading to a radiative decay limit of (4)

$$\tau_\gamma / m_\nu \gtrsim 0.8 \times 10^{15}\ \mathrm{s/eV}. \qquad 6.$$

For higher-mass neutrinos, the photon burst would have been stretched beyond the GRS window. The first γ-rays from decays near the SN would arrive in coincidence with the $\bar{\nu}_e$ burst, but the γ-burst duration would be given by something like Equation 4. As a further complication, such higher-mass neutrinos violate the cosmological mass limit unless they decay sufficiently fast and thus nonradiatively. Put another way, one must simultaneously worry about radiative and nonradiative decay channels (see 4 for a detailed discussion).

Comparable limits in the higher-mass range were also derived from γ-ray data of the Pioneer Venus Orbiter (PVO) (176). For $m_\nu \gtrsim 0.1$ MeV, decay photons still arrive years after SN 1987A. In 1991, the COMPTEL instrument aboard the Compton Gamma Ray Observatory looked at the SN 1987A remnant for about 0.68×10^6 s, providing the most restrictive limits in this mass range (177, 178).

For $m_\nu \gtrsim 2m_e \approx 1.2$ MeV, which is only possible for ν_τ (for which the experimental mass limit is about 18 MeV), the dominant radiative decay channel is $\nu_\tau \to \nu_e e^+ e^-$. From SN 1987A, one would still expect γ-rays from the bremsstrahlung process $\nu_\tau \to \nu_e e^+ e^- \gamma$, leading to interesting limits (172, 176, 179–181).

The decay positrons from past galactic supernovae would be trapped by the galactic magnetic fields and thus linger for up to 10^5 yr. Independently of SN 1987A, measurements of the galactic positron flux thus provide limits on neutrino decays with final-state positrons (4, 182).

4.5 Explosion Energetics

In the standard scenario of a type II SN explosion, a shock wave forms near the edge of the core when its collapse halts at nuclear density, and this shock wave ejects the mantle of the progenitor star. However, in typical numerical calculations, the shock wave stalls, so that this "prompt explosion" scenario does not seem to work. In the "delayed explosion" picture, the shock wave is revived by neutrino

heating, perhaps in conjunction with convection, but even then it appears difficult to obtain a successful or sufficiently energetic explosion.

Therefore, one may speculate that nonstandard modes of energy transfer play an important role. Dirac neutrinos with a magnetic dipole moment of order $10^{-12}\,\mu_{\rm B}$ (Bohr magnetons) are one example. The right-handed (sterile) components would arise in the deep inner core by helicity-flipping collisions and escape. They precess back into interacting states in the large magnetic fields outside the SN core and heat the shock region; their interaction cross section would be relatively large because of their large inner-core energies (183–187; A Dar, unpublished).

Certainly it is important not to deposit too much energy in the mantle and envelope of the star. Ninety-nine percent of the gravitational binding energy of the neutron star goes into neutrinos, about 1% into the kinetic energy of the explosion, and about 0.01% into the optical supernova. Therefore, neutrinos or other particles emitted from the core must not decay radiatively within the progenitor's envelope radius of about 100 s or else too much energy lights up (188, 189).

4.6 Neutrino Spectra and Neutrino Oscillations

Neutrino oscillations can have several interesting ramifications in the context of SN physics because the temporal and spectral characteristics of the emission process depend on the neutrino flavor (90–92, 202). The simplest case is that of the "prompt ν_e burst," which represents the deleptonization of the outer core layers at about 100 ms after bounce, when the shock wave breaks through the edge of the collapsed iron core. This "deleptonization burst" propagates through the mantle and envelope of the progenitor star, so that resonant oscillations take place for a large range of mixing parameters between ν_e and some other flavor, notably for most of those values where the Mikheyev-Smirnov-Wolfenstein (MSW) effect operates in the Sun (190–199). In a water Cherenkov detector, this burst is visible as forward-peaked $\nu_e e$ scattering, but one would have expected only a fraction of an event from SN 1987A. The first event in Kamiokande may be attributed to this signal, but this interpretation is statistically insignificant.

During the next few hundred milliseconds, the shock wave stalls a few hundred kilometers above the core and needs rejuvenating. The efficiency of neutrino heating can be increased by resonant flavor oscillations that swap the ν_e flux with, say, the ν_τ one. Therefore, what passes through the shock wave as a ν_e was born as a ν_τ at the proto–neutron-star surface. It has, on average, higher energies and thus is more effective at transfering energy. In Figure 9, the shaded range of mixing parameters is where supernovae are helped to explode, assuming a "normal" neutrino mass spectrum with $m_{\nu_e} < m_{\nu_\tau}$ (200). Below the shaded region, the resonant oscillations take place beyond the shock wave and thus do not affect the explosion.

The logic of this scenario depends on deviations from strictly thermal neutrino emission at some blackbody neutrino sphere. The neutrino cross sections are very energy-dependent and different for different flavors, so that the concept

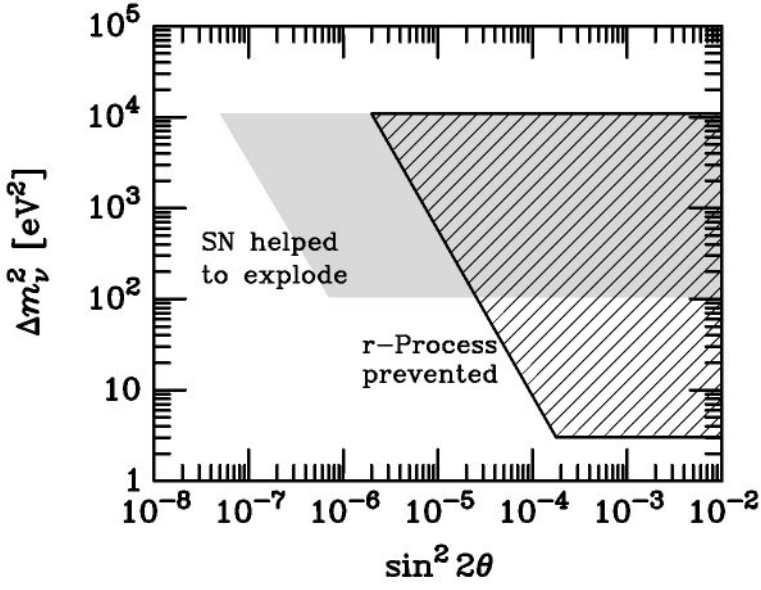

Figure 9 Mass difference and mixing between ν_e and ν_μ or ν_τ, where a spectral swap would occur to help explode supernovae (schematically after Reference 200), and where it would prevent r-process nucleosynthesis (schematically after References 213–215).

of a neutrino sphere is rather crude—the spectra are neither thermal nor equal for the different flavors (201, 202). The dominant opacity source for ν_e is the process $\nu_e + n \rightarrow p + e^-$; for $\overline{\nu}_e$ it is $\overline{\nu}_e + p \rightarrow n + e^+$; and for $\nu_{\mu,\tau}$ and $\overline{\nu}_{\mu,\tau}$ it is neutral-current scattering on nucleons. Therefore, unit optical depth is at the largest radius (and lowest medium temperature) for ν_e, and deepest (highest temperature) for $\nu_{\mu,\tau}$ and $\overline{\nu}_{\mu,\tau}$. In typical calculations, one finds a hierarchy $\langle E_{\nu_e}\rangle : \langle E_{\overline{\nu}_e}\rangle : \langle E_{\text{others}}\rangle \approx \frac{2}{3} : 1 : \frac{5}{3}$ with $\langle E_{\overline{\nu}_e}\rangle = 14$–$17$ MeV (92). The SN 1987A observations imply a somewhat lower range of $\langle E_{\overline{\nu}_e}\rangle \approx 7$–$14$ MeV (96, 99).

It should be noted that, pending a more detailed numerical confirmation (S Hardy, HT Janka, G Raffelt, work in progress), the difference between the $\overline{\nu}_e$ and $\nu_{\mu,\tau}$ or $\overline{\nu}_{\mu,\tau}$ average energies appears to be smaller than is commonly assumed (126, 203–205), but there is no doubt that the ν_e spectrum is softer than the others. Still, the quantitative import of flavor oscillations depends on details of the neutrino spectra formation process in those SN core layers where the diffusion approximation for the neutrino transport is no longer valid, yet neutrinos are still trapped.

A few seconds after core bounce, the shock wave has long since taken off, leaving behind a relatively dilute "hot bubble" above the neutron-star surface. This region is one suspected site for r-process heavy-element synthesis, which requires a neutron-rich environment (206–212). The neutron-to-proton ratio, which is

governed by the β reactions $\nu_e + n \rightarrow p + e^-$ and $\overline{\nu}_e + p \rightarrow n + e^+$, is shifted to a neutron-rich phase if $\langle E_{\nu_e} \rangle < \langle E_{\overline{\nu}_e} \rangle$ as for standard neutrino spectra. Resonant oscillations can again swap the ν_e flux with another one, inverting this hierarchy of energies. In Figure 9, in the hatched range of mixing parameters, the r-process would be disturbed (213–216). On the other hand, $\nu_e \rightarrow \nu_s$ oscillations into a sterile neutrino could actually help the r-process by removing some of the neutron-stealing ν_e (217, 234).

A large body of recent literature was devoted to explaining the large kick velocities of the observed radio pulsars as a "neutrino rocket effect." The required few-percent anisotropy of the neutrino emission from a SN core was attributed to an intricate interplay between the magnetic-field–induced neutrino dispersion relation and resonant oscillations (218–225). However, due to a conceptual error, the effect was vastly overestimated (226), so the pulsar kicks do not seem to be related to neutrino oscillations in any obvious way.

If the mixing angle between ν_e and some other flavor is large, the $\overline{\nu}_e$ flux from a SN contains a significant fraction of oscillated states that were born as $\overline{\nu}_\mu$ or $\overline{\nu}_\tau$ and thus should have higher average energies. The measured SN 1987A event energies are already somewhat low, a problem so strongly exacerbated by oscillations that a large–mixing-angle solution of the solar neutrino deficit poses a problem (99, 104, 227). This conclusion, however, depends on the standard predictions for the average neutrino energies, which may not hold up to closer scrutiny, as mentioned above.

5. LIMITS ON NEUTRINO PROPERTIES

5.1 Masses and Mixing

Astrophysics and cosmology play a fundamental role in neutrino physics, since the properties of stars and the universe at large provide some of the most restrictive limits on nonstandard properties of these elusive particles. Therefore, it behooves me to summarize what the astrophysical arguments introduced in the previous sections teach us about neutrinos.

Unfortunately, stars tell us little about neutrino masses, the holy grail of neutrino physics. The current discourse (228–230) centers on the interpretation of the solar (7) and atmospheric (231) neutrino anomalies and the Liquid Scintillator Neutrino Detector (LSND) experiment (232, 233), all of which provide very suggestive evidence for neutrino oscillations. Solar neutrinos imply a Δm_ν^2 of about 10^{-5} eV^2 (MSW solutions) or 10^{-10} eV^2 (vacuum oscillations), atmospheric neutrinos 10^{-3}–10^{-2} eV^2, and the LSND experiment 0.3–8 eV^2. Taken together, these results require a fourth flavor, a sterile neutrino. This is perhaps the most spectacular implication of these experiments, but it is of course also the least secure one.

Core-collapse supernovae appear to be the only case in stellar astrophysics, apart from the solar neutrino flux, where neutrino oscillations can be important. However, Figure 9 reveals that the experimentally favored mass differences negate

a role of neutrino oscillations for the explosion mechanism or r-process nucleosynthesis, except perhaps when sterile neutrinos exist (217, 234). Oscillations affect the interpretation of the SN 1987A signal (99, 104, 227) and that of a future galactic SN (235–237). However, as discussed in Section 4.6, the main challenge is to develop a quantitatively more accurate understanding of supernovae as neutrino sources before relying on relatively fine points of the neutrino spectral characteristics to learn about neutrino mixing parameters.

Oscillation experiments reveal only mass differences, so one still needs to worry about the absolute neutrino mass scale. The absence of anomalous SN 1987A signal dispersion (Section 4.2) gives a limit (96, 104)

$$m_{\nu_e} \lesssim 20 \text{ eV}, \qquad 7.$$

somewhat weaker than current laboratory bounds. A high-statistics observation of a galactic SN by a detector such as Superkamiokande could improve this limit to something like 3 eV by using the fast rise-time of the neutrino burst as a measure of dispersion effects (238). If the neutrino mass differences are indeed very small, this limit carries over to the other flavors. One can derive an independent mass limit on ν_μ and ν_τ in the range of a few tens of electron volts if one identifies a neutral-current signature in a water Cherenkov detector (239–243), or if a future neutral-current detector provides an additional measurement.

The SN 1987A energy-loss argument (Section 4.3) provides a limit on a neutrino Dirac mass of (4, 120, 145–148, 152)

$$m_\nu(\text{Dirac}) \lesssim 30 \text{ keV}. \qquad 8.$$

It is based on the idea that trapped Dirac neutrinos produce their sterile component with a probability of about $(m_\nu/2E_\nu)^2$ in collisions and thus feed energy into an invisible channel. This result was important in the discourse on Simpson's 17-keV neutrino, which is now of only historical interest (246).

5.2 Dipole and Transition Moments

5.2.1 Electromagnetic Form Factors Neutrino electromagnetic interactions would provide for a great variety of astrophysical implications. In the vacuum, the most general neutrino interaction with the electromagnetic field is (247, 248)

$$\mathcal{L}_{\text{int}} = -F_1\bar{\psi}\gamma_\mu\psi A^\mu - G_1\bar{\psi}\gamma_\mu\gamma_5\psi\partial_\mu F^{\mu\nu} - \tfrac{1}{2}\bar{\psi}\sigma_{\mu\nu}(F_2 + G_2\gamma_5)\psi F^{\mu\nu}, \quad 9.$$

where ψ is the neutrino field, A^μ is the electromagnetic vector potential, and $F^{\mu\nu}$ is the field-strength tensor. The form factors are functions of Q^2, with Q the energy-momentum transfer. In the $Q^2 \to 0$ limit, F_1 is the electric charge, G_1 an anapole moment, F_2 a magnetic moment, and G_2 an electric dipole moment.

Even if neutrinos are electrically strictly neutral, so that $F_1(0) = 0$, they still have a charge radius, usually defined as $\langle r^2\rangle = 6\partial F_1(Q^2)/e\partial Q^2|_{Q^2=0}$. This form factor provides for a contact interaction, not for a long-range force, and as such

modifies processes with Z^0 exchange (249–253). Because astrophysics provides no precision test for the effective strength of neutral-current interactions, this form factor is best probed in laboratory experiments (254). Likewise, the anapole interaction vanishes in the $Q^2 \to 0$ limit and thus represents a modification to the standard neutral-current interaction, with no apparent astrophysical consequences.

The most interesting possibilities are magnetic and electric dipole and transition moments. If the standard model is extended to include neutrino Dirac masses, the magnetic dipole moment is $\mu_\nu = 3.20 \times 10^{-19}\,\mu_{\rm B}\,m_\nu/{\rm eV}$, where $\mu_{\rm B} = e/2m_e$ is the Bohr magneton (247, 248). An electric dipole moment ϵ_ν violates CP, and both are forbidden for Majorana neutrinos. Including flavor mixing implies electric and magnetic transition moments for both Dirac and Majorana neutrinos, but they are even smaller due to a Glashow-Iliopoulos-Maiani (GIM) cancellation. These values are far too small to be of any experimental or astrophysical interest. Significant neutrino electromagnetic form factors require a more radical extension of the standard model, e.g. the existence of right-handed currents.

5.2.2 Plasmon Decay in Stars Dipole or transition moments allow several interesting processes (Figure 10). For the purpose of deriving limits, the most important case is $\gamma \to \nu\bar{\nu}$, which is kinematically possible in a plasma because the photon acquires a dispersion relation that roughly amounts to an effective mass. Even without anomalous couplings, the plasmon decay proceeds because the charged particles of the medium induce an effective neutrino-photon interaction. Put another way, even standard neutrinos have nonvanishing electromagnetic form factors in a medium (255, 256). The standard plasma process (257–259) dominates the neutrino production in white dwarfs or the cores of globular-cluster red giants.

The plasma process was first used to constrain neutrino electromagnetic couplings (260). (See 29, 35, 37, 73 for numerical implementations of the nonstandard rates in stellar-evolution calculations.) The helium-ignition argument in globular clusters (Section 3.1.2), equivalent to Equation 2, implies a limit (4, 28, 36, 37)

$$\mu_\nu \lesssim 3 \times 10^{-12}\,\mu_{\rm B}, \qquad 10.$$

applicable to magnetic and electric dipole and transition moments for Dirac and Majorana neutrinos. Of course, the final-state neutrinos must be lighter than the photon plasma mass, which is around 10 keV for the relevant conditions.

The corresponding laboratory limits are much weaker (3). The most restrictive bound is $\mu_{\nu_e} < 1.8 \times 10^{-10}\,\mu_{\rm B}$ at 90% CL from a measurement of the $\bar{\nu}_e e$ scattering cross section involving reactor sources. A significant improvement should become possible with the MUNU experiment (261), but it is unlikely that the globular-cluster limit can be reached any time soon.

5.2.3 Radiative Decay A neutrino mass eigenstate ν_i may decay to another one ν_j by the emission of a photon, where the only contributing form factors are the

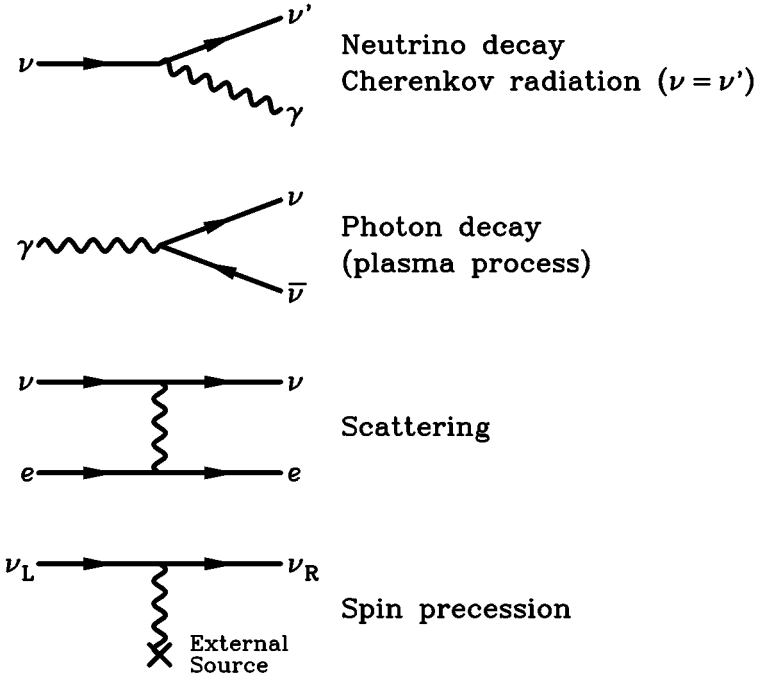

Figure 10 Processes with neutrino electromagnetic dipole or transition moments.

magnetic and electric transition moments. The inverse radiative lifetime is found to be (247, 248)

$$\tau_\gamma^{-1} = \frac{|\mu_{ij}|^2 + |\epsilon_{ij}|^2}{8\pi}\left(\frac{m_i^2 - m_j^2}{m_i}\right)^3 = 5.308\ \mathrm{s}^{-1}\left(\frac{\mu_{\rm eff}}{\mu_{\rm B}}\right)^2\left(\frac{m_i^2 - m_j^2}{m_i^2}\right)^3\left(\frac{m_i}{\rm eV}\right)^3, \qquad 11.$$

where μ_{ij} and ϵ_{ij} are the transition moments while $|\mu_{\rm eff}|^2 \equiv |\mu_{ij}|^2 + |\epsilon_{ij}|^2$. Radiative neutrino decays have been constrained from the absence of decay photons of reactor $\overline{\nu}_e$ fluxes (262), the solar ν_e flux (263, 264), and the SN 1987A neutrino burst (171–175). For $m_\nu \equiv m_i \gg m_j$, these limits can be expressed as

$$\frac{\mu_{\rm eff}}{\mu_{\rm B}} \lesssim \begin{cases} 0.9 \times 10^{-1}\ (\mathrm{eV}/m_\nu)^2 & \text{Reactor } (\overline{\nu}_e), \\ 0.5 \times 10^{-5}\ (\mathrm{eV}/m_\nu)^2 & \text{Sun } (\nu_e), \\ 1.5 \times 10^{-8}\ (\mathrm{eV}/m_\nu)^2 & \text{SN 1987A (all flavors)}, \\ 1.0 \times 10^{-11}\ (\mathrm{eV}/m_\nu)^{9/4} & \text{Cosmic background (all flavors)}. \end{cases} \qquad 12.$$

In this form, the SN 1987A limit applies for $m_\nu \lesssim 40$ eV, as explained in Section 4.4. The decay of cosmic background neutrinos would contribute to the diffuse photon backgrounds, excluding the shaded areas in Figure 11. They are approximately

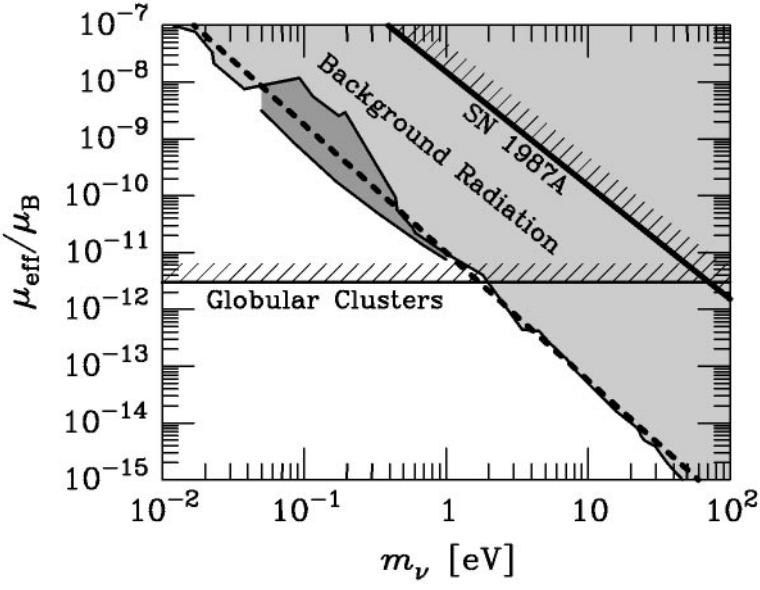

Figure 11 Astrophysical limits on neutrino dipole moments. Light-shaded background-radiation limits are from Reference 265; dark-shaded ones from Reference 266, 267; dashed line is the approximation formula in Equation 12, bottom line.

delineated by the dashed line, corresponding to the bottom line in Equation 12. More restrictive limits obtain for certain masses above 3 eV from the absence of emission features from several galaxy clusters (268, 269, 385).

For low-mass neutrinos, the m_ν^3 phase-space factor in Equation 11 is so punishing that the globular-cluster limit is the most restrictive one for m_ν below a few electron volts. This is precisely the mass range that currently appears favored from neutrino oscillation experiments. Turning this around, the globular-cluster limit implies that radiative decays of low-mass neutrinos do not seem to have observable consequences.

For masses above about 30 eV, one must invoke fast invisible decays in order to avoid a conflict with the cosmological mass limit. In this case, radiative decay limits involve the total lifetime as another parameter; the SN 1987A limits have been interpreted in this sense (4, 174, 176, 178).

5.2.4 Cherenkov Effect Another form of "radiative decay" is the Cherenkov effect $\nu \to \nu + \gamma$, which involves the same initial- and final-state neutrino. This process is kinematically allowed for photons with $\omega^2 - \mathbf{k}^2 < 0$, which obtains in certain media or in external magnetic fields. The neutrino may have an anomalous dipole moment, but there is also a standard-model photon coupling induced by the medium or the external field. Thus far, it does not look as if the neutrino

Cherenkov effect has any strong astrophysical significance (see 270 for a review of the literature).

5.2.5 Spin-Flip Scattering The magnetic or electric dipole interaction couples neutrino fields of opposite chirality. In the relativistic limit, this implies that a neutrino flips its helicity in an "electromagnetic collision," which in the Dirac case produces the sterile component. The active states are trapped in a SN core, so that spin-flip collisions open an energy-loss channel in the form of sterile states. Conversely, the SN 1987A energy-loss argument (Section 4.3) allows one to derive a limit (163, 166),

$$\mu_\nu(\text{Dirac}) \lesssim 3 \times 10^{-12}\,\mu_\text{B}, \qquad 13.$$

for both electric and magnetic dipole and transition moments. It is the same as the globular-cluster limit, Equation 10, which however includes the Majorana case.

Spin-flip collisions would also populate the sterile Dirac components in the early universe and thus increase the effective number of thermally excited neutrino degrees of freedom. Full thermal equilibrium is attained for $\mu_\nu(\text{Dirac}) \gtrsim 60 \times 10^{-12}\,\mu_\text{B}$ (34, 271). In view of the SN 1987A and globular-cluster limits, this result assures us that big-bang nucleosynthesis remains undisturbed.

5.2.6 Spin and Spin-Flavor Precession Neutrinos with magnetic or electric dipole moments spin-precess in external magnetic fields (272, 273). For example, solar neutrinos can precess into sterile and thus undetectable states in the Sun's magnetic field (274–276). The same is true of SN neutrinos in the galactic magnetic field, where an important effect obtains for $\mu_\nu \gtrsim 10^{-12}\,\mu_\text{B}$. Moreover, the high-energy sterile states emitted by spin-flip collisions from the inner SN core could precess back into active ones and cause events with anomalously high energies in SN neutrino detectors, an effect that probably requires $\mu_\nu(\text{Dirac}) \lesssim 10^{-12}\,\mu_\text{B}$ from the SN 1987A signal (163, 277). For the same general μ_ν magnitude, one may expect an anomalous rate of energy transfer to the shock wave in a SN, helping with the explosion (Section 4.5).

In a medium, the refractive energy shift for active neutrinos relative to sterile ones creates a barrier to the spin precession (279, 280). The mass difference has the same effect if the precession is between different flavors through a transition moment (278). However, the mass and refractive terms may cancel, leading to resonant spin-flavor oscillations in the spirit of the MSW effect (281–284). This mechanism can explain all solar neutrino data (285, 286) but requires rather large toroidal magnetic fields in the Sun, since the neutrino magnetic (transition) moments have to obey the globular-cluster limit of Equation 10. For Majorana neutrinos, the spin-flavor precession amounts to transitions between neutrinos and antineutrinos, so that the observation of antineutrinos from the Sun would be a diagnostic for this effect (287–289).

Large magnetic fields exist in SN cores, so spin-flavor precession could play an important role there, with possible consequences for the explosion mechanism, r-process nucleosynthesis, or the measurable neutrino signal (290–294). The downside of this richness of phenomena is that there are so many unknown parameters (electromagnetic neutrino properties, masses, mixing angles), as well as the unknown magnetic field strength and distribution, that it is difficult to come up with reliable limits or requirements on neutrino properties. The SN phenomenon is probably too complicated to serve as a laboratory to pin down electromagnetic neutrino properties, but it clearly is an environment where these properties could have far-reaching consequences.

5.3 Millicharged Particles

It is conceivable that neutrinos carry small electric charges if charge conservation is not exact (295, 296) or if the families are not sequential (297–299). Moreover, new particles with small electric charges are motivated in certain models with a "mirror sector" and a slightly broken mirror symmetry (300). Therefore, it is interesting to study the experimental, astrophysical, and cosmological bounds on "millicharged" particles (301–305).

A model-independent ν_e charge limit arises from the absence of dispersion of the SN 1987A neutrino signal in the galactic magnetic field (5, 105),

$$e_{\nu_e} \lesssim 3 \times 10^{-17}\, e. \qquad 14.$$

If charge conservation holds in neutron decay, $e_{\nu_e} \lesssim 3 \times 10^{-21}\, e$ results, based on a limit for the neutron charge of $e_n = (-0.4 \pm 1.1) \times 10^{-21}\, e$ (306) and on the neutrality of matter, which was found to be $e_p + e_e = (0.8 \pm 0.8) \times 10^{-21}\, e$ (307). The measured ν_μ-e cross section implies $e_{\nu_\mu} \lesssim 10^{-9}\, e$ (303).

Generic millicharged particles (charge e_x, mass m_x) could appear as virtual states and would thus modify the Lamb shift unless $e_x < 0.11 e\, m_x/\mathrm{MeV}$ (302). A number of limits follow from a host of previous accelerator experiments (302) and a recent dedicated search at SLAC (308) (see Figure 12).

Millicharged particles are produced by the plasmon decay process and thus drain energy from stars. In globular clusters, the emission rate is almost the same for HB stars and red giants before helium ignition, in contrast with the magnetic-dipole case. Therefore, Equations 2 and 3 give an almost identical limit (259),

$$e_x \lesssim 2 \times 10^{-14}\, e, \qquad 15.$$

applicable for m_x below a few kilo-electron-volts. The SN 1987A energy-loss argument extends the exclusion range to about 10 MeV for $10^{-9}\, e \lesssim e_x \lesssim 10^{-7}\, e$ (4, 167).

The usual big-bang nucleosynthesis limit on the effective number of neutrino species N_{eff} provides another constraint. A millicharged neutrino is of Dirac nature, so its right-handed component adds one effective species. If the millicharged particles are not neutrinos, then, depending on their spin, N_{eff} may increase even more.

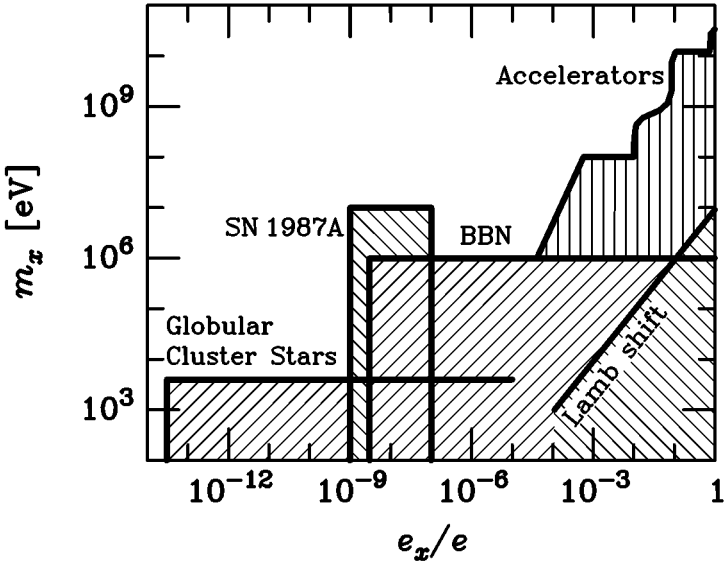

Figure 12 Limits on the electric charge e_x and mass m_x of generic millicharged particles that may be neutrinos or new particles. In order to avoid overclosing the universe, additional model-dependent parameter regions are excluded. The big-bang nucleosynthesis (BBN) excluded region is larger in some models.

If big-bang nucleosynthesis excludes one extra species, one finds $e_x \lesssim 3 \times 10^{-9}\, e$ for $m_x \lesssim 1$ MeV (302). More stringent limits apply in certain models where the millicharged particles are associated with a shadow sector (305).

Further regions in Figure 12 are excluded to avoid "overclosing" of the universe by the new particles (302, 305). However, because their relic density depends on their annihilation cross section, it is necessary to specify a model. It is hard to imagine new particles that interact solely through their small electric charge.

5.4 Nonstandard Weak Interactions

5.4.1 Right-Handed Currents Right-handed (r.h.) weak interactions may exist on some level, e.g. in left-right symmetric models where the r.h. gauge bosons differ from the standard ones by their mass. In the low-energy limit relevant for stars, one may account for the new couplings by a r.h. Fermi constant $\epsilon G_{\rm F}$, where ϵ is a small, dimensionless parameter. In left-right symmetric models, one finds explicitly for charged-current processes $\epsilon_{\rm CC}^2 = \zeta^2 + [m(W_L)/m(W_R)]^2$, where $m(W_{L,R})$ are the l.h. and r.h. gauge boson masses and ζ is the left-right mixing parameter (158).

Assuming that neutrinos are Dirac particles, a SN core loses energy into r.h. states as an "invisible channel" by the process $e + p \to n + \nu_{e,R}$. The SN 1987A

energy-loss argument (Section 4.3) then requires $\epsilon_{\rm CC} \lesssim 10^{-5}$ (4, 120, 158). Laboratory experiments yield a weaker limit of order $\epsilon_{\rm CC} \lesssim 3 \times 10^{-2}$ (309) but do not depend on the assumed existence of r.h. neutrinos.

For neutral currents, the dominant emission process is $NN \to NN\nu_R\bar{\nu}_R$, which is subject to saturation effects, as in the case of axion emission (126). One then finds $\epsilon_{\rm NC} \lesssim 3 \times 10^{-3}$ (4), somewhat less restrictive than the original limits (120, 158; see also 159–161). This bound is also somewhat less restrictive than $\epsilon_{\rm NC} \lesssim 10^{-3}$ found from big-bang nucleosynthesis (310).

5.4.2 Secret Neutrino Interactions and Majorons The neutrino-neutrino cross section is not known experimentally. It could be anomalously large if neutrino Majorana masses were to arise from a suitable majoron model (311–314). "Secret" neutrino-neutrino interactions were constrained by the fact that the SN 1987A neutrino signal was not depleted by collisions with cosmic background neutrinos (315). Supernova physics with majorons and SN 1987A limits were discussed in the literature (128–134, 316–321). There is little doubt that majoron models will have an important impact on SN physics for neutrino-majoron Yukawa couplings in the 10^{-6}–10^{-3} range. The existing literature, however, is too confusing for this author to come up with a clear synthesis of what SN physics implies for majoron models.

5.4.3 Flavor-Changing Neutral Currents In certain models, the neutrino neutral current has an effective flavor-changing component. Neutrinos propagating in matter then have medium-induced mixings and thus can oscillate even if they are strictly massless (322, 323). Naturally, this phenomenon can be important for the oscillation of solar (324–327) and supernova (328, 329) neutrinos.

6. AXIONS AND OTHER PSEUDOSCALARS

6.1 Interaction Structure

New spontaneously broken global symmetries imply the existence of Nambu-Goldstone bosons that are massless and as such present the most natural case (besides neutrinos) for using stars as particle-physics laboratories. Massless scalars would lead to new long-range forces (Section 7), so we may focus here on pseudoscalars. The most prominent example, axions, were proposed more than 20 years ago as a solution to the strong *CP* problem (330–333; see 334, 335 for reviews and 336 for the latest developments). We use axions as a generic example; it will be obvious how to extend the following results and discussions to other cases.

Actually, axions are only pseudo–Nambu-Goldstone bosons, in that the spontaneously broken chiral Peccei-Quinn symmetry $U_{\rm PQ}(1)$ is also explicitly broken, providing these particles with a small mass

$$m_a = 0.60\ {\rm eV}\frac{10^7\ {\rm GeV}}{f_a}. \qquad 16.$$

Here, f_a is the Peccei-Quinn scale, an energy scale that is related to the vacuum expectation value of the field that breaks $U_{\rm PQ}$ (1). The properties of Nambu-Goldstone bosons are always related to such a scale, which is the main quantity to be constrained by astrophysical arguments, whereas Equation 16 is specific to axions and allows the expression of limits on f_a in terms of m_a.

In order to calculate the axionic energy-loss rate from stellar plasmas, it is necessary to specify the interaction with the medium constituents. The interaction with a fermion j (mass m_j) is generically

$$\mathcal{L}_{\rm int} = \frac{C_j}{2\,f_a}\,\bar{\Psi}_j\gamma^\mu\gamma_5\Psi_j\partial_\mu a \quad \text{or} \quad -i\,\frac{C_j m_j}{f_a}\,\bar{\Psi}_j\gamma_5\Psi_j a, \qquad 17.$$

where Ψ_j is the fermion and a the axion field, and C_j is a model-dependent coefficient of order unity. The combination $g_{aj} \equiv C_j m_j/f_a$ plays the role of a Yukawa coupling, and $\alpha_{aj} \equiv g_{aj}^2/4\pi$ acts as an "axionic fine structure constant." The derivative form of the interaction is more fundamental in that it is invariant under $a \to a + a_0$ and thus respects the Nambu-Goldstone nature of these particles. The pseudoscalar form is usually equivalent, but one has to be careful when calculating processes where two Nambu-Goldstone bosons are attached to one fermion line, e.g. an axion and a pion attached to a nucleon (120, 337–340).

The dimensionless couplings C_i depend on the detailed implementation of the Peccei-Quinn mechanism. Limiting the present discussion to "invisible axion models" where f_a is much larger than the scale of electroweak symmetry breaking, it is conventional to distinguish between models of the DFSZ type [for Dine, Fischler, Srednicki (341), Zhitnitskiĭ (342)] and of the KSVZ type [for Kim (343), Shifman, Vainshtein, Zakharov (344)]. In KSVZ models, axions have no tree-level couplings to the standard quarks or leptons, yet axions couple to nucleons by their generic mixing with the neutral pion. The latest analysis gives numerically (127)

$$C_p = -0.34, \quad C_n = 0.01, \qquad 18.$$

with a statistical uncertainty of about ± 0.04 and an estimated systematic uncertainty of roughly the same magnitude. The tree-level couplings to standard quarks and leptons in the DFSZ model depend on an angle β that measures the ratio of vacuum expectation values of two Higgs fields. One finds (127)

$$C_e = \tfrac{1}{3}\cos^2\beta, \quad C_p = -0.07 - 0.46\cos^2\beta, \quad C_n = -0.15 + 0.38\cos^2\beta, \qquad 19.$$

with uncertainties similar to those of the KSVZ case.

The *CP*-conserving interaction between photons and pseudoscalars is commonly expressed in terms of an inverse energy scale $g_{a\gamma}$ according to

$$\mathcal{L}_{\rm int} = \tfrac{1}{4} g_{a\gamma} F_{\mu\nu}\tilde{F}^{\mu\nu} a = -g_{a\gamma}\mathbf{E}\cdot\mathbf{B}\,a, \qquad 20.$$

where F is the electromagnetic field-strength tensor and $\tilde{F}$ is its dual. For axions,

$$g_{a\gamma} = \frac{\alpha}{2\pi f_a}\,C_\gamma, \quad C_\gamma = \frac{E}{N} - 1.92 \pm 0.08, \qquad 21.$$

where E/N is the ratio of the electromagnetic and color anomalies, a model-dependent ratio of small integers. In the DFSZ model or grand unified models, one has $E/N = 8/3$, for which $C_\gamma \approx 0.75$, but one can also construct models with $E/N = 2$, which significantly reduces the axion-photon coupling (345). (See 346, 347 for reviews of the value of C_γ in a great variety of cases.)

6.2 Limits on the Interaction Strength

6.2.1 Photons The interaction of axions with fermions or photons allows numerous reactions that can produce axions in stars, which may imply limits on the axion coupling strength. Beginning with photons, pseudoscalars interact according to the Lagrangian of Equation 20, which allows the decay $a \to 2\gamma$. In stellar plasmas, the photon-axion interaction also makes possible the Primakoff conversion $\gamma \leftrightarrow a$ in the electric fields of electrons and nuclei (38)—see Figure 1. For low-mass pseudoscalars, the emission rate was calculated for various degrees of electron degeneracy (48, 74, 348), superseding an earlier calculation in which screening effects had been ignored (43).

The helioseismological constraint on solar energy losses then leads to Equation 1 as a bound on $g_{a\gamma}$. Figure 13 ("Sun") shows this constraint in the context of

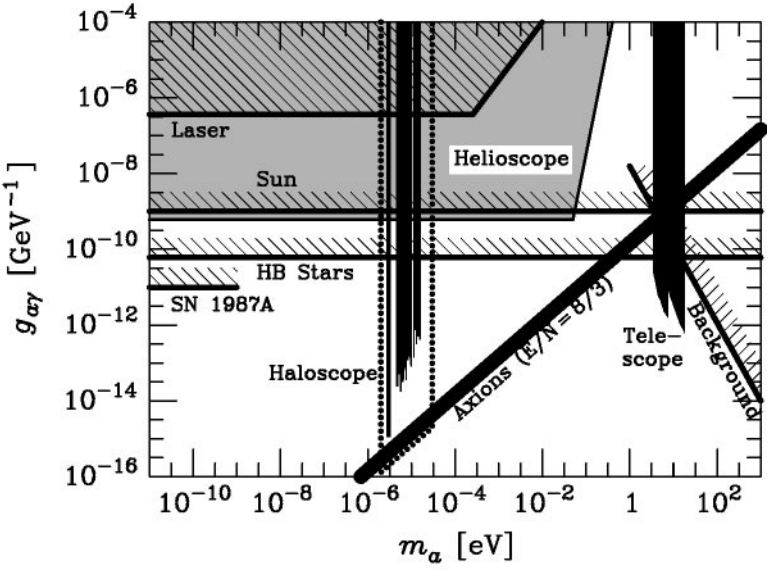

Figure 13 Limits to the axion-photon coupling $g_{a\gamma}$ as defined in Equation 20. They apply to any pseudoscalar, except for the "haloscope" search, which assumes that these particles are the galactic dark matter; the dotted region marks the projected sensitivity range of the ongoing dark-matter axion searches. For higher masses than those shown here, the pertinent limits are reviewed in Reference 350.

other bounds; similar plots are found in References 3, 4, 349–351. For axions, the relationship between $g_{a\gamma}$ and m_a is indicated by the heavy solid line, assuming $E/N = 8/3$.

It is also possible to search directly for solar axions. One method ("helioscope") is to direct a dipole magnet toward the Sun, allowing solar axions to mutate into X-rays by the inverse Primakoff process (353, 354). A pilot experiment was not sensitive enough (355), but the exposure time was significantly increased in a new experiment in Tokyo, where a dipole magnet was gimballed like a telescope so that it could follow the Sun (356, 357). The resulting limit $g_{a\gamma} \lesssim 6 \times 10^{-10}$ GeV^{-1} is more restrictive than Equation 1. Another helioscope project was begun in Novosibirsk several years ago (359), but its current status has not been reported for some time. An intriguing project (SATAN) at CERN would use a decommissioned Large Hadron Collider (LHC) test magnet that could be mounted on a turning platform to achieve reasonable periods of alignment with the Sun (360). This setup could begin to compete with the globular-cluster limit of Equation 22.

The axion-photon transition in a macroscopic magnetic field is analogous to neutrino oscillations and thus depends on the particle masses (358). For a large mass difference, the transition is suppressed by the momentum mismatch of particles with equal energies. Therefore, the Tokyo limit applies only for $m_a \lesssim 0.03$ eV. A next step will be to fill the helioscope with a pressurized gas, giving the photon a dispersive mass to overcome the momentum mismatch.

An alternative method is Bragg diffraction, which uses the strong electric field of a crystal lattice that has large Fourier components for the required momentum transfer (361–363). The experiment has been performed using Ge detectors, originally built to search for neutrinoless double-β decay and for WIMP dark matter; the crystal serves simultaneously as a Primakoff "transition agent" and as an X-ray detector. A first limit of the SOLAX Experiment (364) of $g_{a\gamma} \lesssim 27 \times 10^{-10}$ GeV^{-1} is not yet compatible with Equation 1 and thus not self-consistent. In the future, this limit may be reached, but prospects of going much further appear dim (365).

The Primakoff conversion of stellar axions can also proceed in the magnetic fields of sunspots or in the galactic magnetic field, so that one might expect anomalous X- or γ-ray fluxes from the Sun (366), the red supergiant Betelgeuse (367), or SN 1987A (368, 369). Observations of SN 1987A yield $g_{a\gamma} \lesssim 0.1 \times 10^{-10}$ GeV^{-1} for nearly massless pseudoscalars with $m_a \lesssim 10^{-9}$ eV. A similar limit obtains from the isotropy of the cosmic X-ray background, which would be modified by the conversion to axions in the galactic magnetic field (370). Axion-photon conversion in the magnetic fields of stars, the galaxy, or the early universe have also been studied (358, 371–378), but no additional limits have emerged.

The existence of massless pseudoscalars would cause a photon birefringence effect in pulsar magnetospheres, leading to a differential time delay between photons of opposite helicity that limits $g_{a\gamma} \lesssim 0.5 \times 10^{-10}$ GeV^{-1} (379).

A laser beam in a laboratory magnetic field would also be subject to vacuum birefringence (380), adding to the QED Cotton-Mouton effect. First pilot experiments (351, 381) did not reach the QED level. Two vastly improved current projects

are expected to get there (382, 383), but they will stay far away from the "axion line" in Figure 13. With a laser beam in a strong magnet, one can also search for Primakoff axion production and subsequent back-conversion, but a pilot experiment naturally did not have the requisite sensitivity (384). The exclusion range of current laser experiments is schematically indicated in Figure 13.

The most important limit on the photon coupling of pseudoscalars derives from the helium-burning lifetime of HB stars in globular clusters (i.e. from Equation 3),

$$g_{a\gamma} \lesssim 0.6 \times 10^{-10}\ \mathrm{GeV}^{-1}. \qquad 22.$$

For $m_a \gtrsim 10$ keV, this limit quickly degrades as the emission is suppressed when the particle mass exceeds the stellar temperature. For a fixed temperature, the Primakoff energy-loss rate decreases with increasing density, so that Equation 2 implies a less restrictive constraint. Equation 22 was first stated in Reference 4, superseding the slightly less restrictive but often-quoted red-giant bound of Reference 18 (see the discussion after Equation 3). The axion relations of Equations 16 and 21 lead to

$$m_a C_\gamma \lesssim 0.3\ \mathrm{eV} \quad \text{and} \quad f_a/C_\gamma \gtrsim 2 \times 10^7\ \mathrm{GeV}. \qquad 23.$$

In the DFSZ model and grand unified models, $C_\gamma \approx 0.75$, so that $m_a \lesssim 0.4$ eV and $f_a \gtrsim 1.5 \times 10^7$ GeV (Figure 14). For models in which $E/N = 2$ and thus C_γ is very small, the bounds are significantly weaker.

On the basis of their two-photon coupling alone, pseudoscalars can reach thermal equilibrium in the early universe. Their subsequent $a \to 2\gamma$ decays would contribute to the cosmic photon backgrounds (350, 352), excluding a nontrivial m_a-$g_{a\gamma}$ range (Figure 13). Some of the pseudoscalars would end up in galaxies and clusters of galaxies. Their decay would produce an optical line feature that was not found (385, 387), leading to the "telescope" limits in Figure 13. For axions, the telescope limits exclude an approximate mass range 4–14 eV even for a small C_γ.

Axions with a mass in the μeV (10^{-6} eV) range could be the dark matter of the universe (Section 6.3). The Primakoff conversion in a microwave cavity placed in a strong magnetic field ("haloscope") allows one to search for galactic dark-matter axions (353). Two pilot experiments (388, 389) and first results from a full-scale search (390) already exclude a range of coupling strength shown in Figure 13. The new generation of full-scale experiments (336, 390–392) should cover the dotted area in Figure 13, perhaps leading to the discovery of axion dark matter.

6.2.2 Electrons Pseudoscalars that couple to electrons are produced by the Compton process $\gamma + e^- \to e^- + a$ (39, 44, 46, 48, 49, 52) and by the electron bremsstrahlung process $e^- + (A, Z) \to (A, Z) + e^- + a$ (45, 48, 50, 70, 71, 74, 77). A standard solar model yields an axion luminosity of (48) $L_a = \alpha_{ae}\, 6.0 \times 10^{21}\, L_\odot$, where α_{ae} is the axion electron "fine-structure constant" as defined after Equation 17. The helioseismological constraint $L_a \lesssim 0.1\, L_\odot$ of Section 2.3 implies $\alpha_{ae} \lesssim 2 \times 10^{-23}$. White-dwarf cooling gives (4, 69) $\alpha_{ae} \lesssim 1.0 \times 10^{-26}$, while the most restrictive limit is from the delay of helium ignition in low-mass

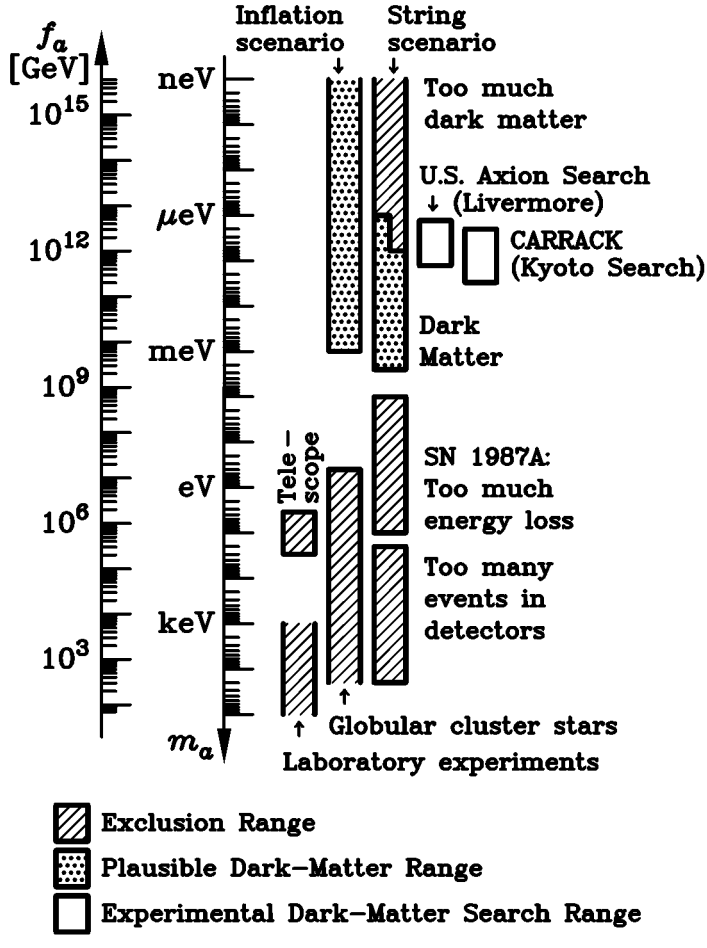

Figure 14 Astrophysical and cosmological exclusion regions (hatched) for the axion mass m_a, or equivalently the Peccei-Quinn scale f_a. The globular-cluster limit depends on the axion-photon coupling; it was assumed that $E/N = 8/3$ as in grand unified models or the DFSZ model. The SN 1987A limits depend on the axion-nucleon couplings; the case shown corresponds to the KSVZ model and approximately to the DFSZ model. The "inclusion regions" (dotted) indicate where axions could plausibly be the cosmic dark matter. Most of the allowed range in the inflation scenario requires fine-tuned initial conditions. In the string scenario, the plausible dark-matter range is somewhat controversial, as indicated by the step in the low-mass end of the "inclusion bar." Also shown is the projected sensitivity range of the search experiments for galactic dark-matter axions.

red giants (52), in the spirit of Equation 2:

$$\alpha_{ae} \lesssim 0.5 \times 10^{-26} \quad \text{or} \quad g_{ae} \lesssim 2.5 \times 10^{-13}. \qquad 24.$$

For $m_a \gtrsim T \approx 10$ keV, this limit quickly degrades because the emission from a thermal plasma is suppressed. The axion relations of Equations 16 and 17 now lead to

$$m_a C_e \lesssim 0.003 \text{ eV} \quad \text{and} \quad f_a/C_e \gtrsim 2 \times 10^9 \text{ GeV}. \qquad 25.$$

In KSVZ-type models, $C_e = 0$ at tree level, so that no interesting limit obtains. In the DFSZ model, $m_a \cos^2\beta \lesssim 0.01$ eV and $f_a/\cos^2\beta \gtrsim 0.7 \times 10^9$ GeV. Because $\cos^2\beta$ can be very small, there is no generic limit on m_a.

6.2.3 Nucleons The axion-nucleon coupling strength is primarily constrained by the SN 1987A energy-loss argument (119–127). The main problem is to estimate the axion emission rate reliably. In the early papers, it was based on a somewhat naive calculation of the bremsstrahlung process $NN \to NNa$, using quasi-free nucleons that interact perturbatively through a one-pion exchange potential. Assuming an equal axion coupling g_{aN} to protons and neutrons, this treatment leads to the g_{aN}-dependent shortening of the SN 1987A neutrino burst of Figure 8. However, in a dense medium, the bremsstrahlung process probably saturates, reducing the naive emission rate by as much as an order of magnitude (126). With this correction, and assuming that the neutrino burst was not shortened by more than half, one reads from Figure 8 an excluded range,

$$3 \times 10^{-10} \lesssim g_{aN} \lesssim 3 \times 10^{-7}. \qquad 26.$$

With Equation 17, this implies an exclusion range of

$$0.002 \text{ eV} \lesssim m_a C_N \lesssim 2 \text{ eV} \quad \text{and} \quad 3 \times 10^6 \text{ GeV} \lesssim f_a/C_N \lesssim 3 \times 10^9 \text{ GeV}. \qquad 27.$$

For KSVZ axions, the coupling to neutrons disappears, whereas the coupling to protons is $C_p \approx -0.34$. With a proton fraction of about 0.3, one estimates an effective $C_N \approx 0.2$, so (4, 126)

$$0.01 \text{ eV} \lesssim m_a \lesssim 10 \text{ eV} \quad \text{and} \quad 0.6 \times 10^6 \text{ GeV} \lesssim f_a \lesssim 0.6 \times 10^9 \text{ GeV} \qquad 28.$$

is excluded.

A detailed numerical study has implemented the values for C_n and C_p appropriate for the KSVZ model and for the DFSZ model with different choices of $\cos^2\beta$ (127). For KSVZ axions one finds a limit $m_a \lesssim 0.008$ eV, whereas for DFSZ axions it varies between about 0.004 and 0.012 eV, depending on $\cos^2\beta$. In view of the large overall uncertainties, it is probably good enough to remember $m_a \lesssim 0.01$ eV as a generic limit (Figure 14).

Axions on the strong-interaction side of the exclusion range of Equation 26 would have produced excess counts in the neutrino detectors by their absorption on oxygen if $1 \times 10^{-6} \lesssim g_{aN} \lesssim 1 \times 10^{-3}$ (168). For KSVZ axions, this crudely translates into 20 eV $\lesssim m_a \lesssim 20$ keV as an exclusion range (Figure 14).

6.2.4 Hadronic Axion Window This limit and the "trapping side" of the energy-loss argument have not been studied in as much detail because the relevant m_a range is already excluded by the globular-cluster argument (Figure 14). That argument, however, depends on the axion-photon interaction, which would nearly vanish in models with $E/N = 2$. In this case, a narrow gap of allowed axion masses in the neighborhood of 10 eV may exist between the two SN arguments ("hadronic axion window").

In this region it is possible to derive interesting limits from globular-cluster stars, where axions can be emitted by nuclear processes, causing a metallicity-dependent modification of the core mass at helium ignition (51). It is intriguing that in this window axions could play a cosmological role as a hot dark-matter component (393). (Usually axions are a cold dark-matter candidate.) Moreover, in this window it may be possible to detect a 14.4-keV monochromatic solar axion line that is produced by transitions between the first excited and ground states of ^{57}Fe. In the laboratory, one can then search for axion absorption, which would give rise to X-rays as ^{57}Fe deexcites (394). A recent pilot experiment did not have enough sensitivity to find axions (395), but a vastly improved detector is now in preparation in Tokyo (S Moriyama and M Minowa, personal communication).

6.3 Cosmological Limits

The astrophysical axion mass limits are particularly interesting when juxtaposed with the cosmological ones. For $f_a \gtrsim 10^8$ GeV, cosmic axions never reach thermal equilibrium in the early universe. They are produced by a nonthermal mechanism that is intimately intertwined with their Nambu-Goldstone nature and implies that their contribution to the cosmic density is proportional to $f_a^{1.175}$ and thus to $m_a^{-1.175}$. The requirement not to overclose the universe with axions thus leads to a lower mass limit.

One must distinguish between two generic cosmological scenarios. If inflation occurred after the Peccei-Quinn symmetry breaking or if $T_{\rm reheat} < f_a$, the initial axion field takes on a constant value of $a_{\rm i} = f_a\Theta_{\rm i}$ throughout the universe, where $0 \leq \Theta_{\rm i} < \pi$ is the initial "misalignment" of the QCD Θ parameter (396–399). If $\Theta_{\rm i} \sim 1$, one obtains a critical density in axions for $m_a \sim 1$ μeV, but since $\Theta_{\rm i}$ is unknown, there is no strict cosmological limit on m_a. However, the possibility of fine-tuning $\Theta_{\rm i}$ is limited by inflation-induced quantum fluctuations, which in turn lead to temperature fluctuations of the cosmic microwave background (400–403). In a broad class of inflationary models, one thus finds an upper limit to m_a where axions could be the dark matter. According to the most recent discussion (403), it is about 10^{-3} eV (Figure 14).

If inflation did not occur at all or if it occurred before the Peccei-Quinn symmetry breaking with $T_{\rm reheat} > f_a$, cosmic axion strings form by the Kibble mechanism (404, 405). Their motion is damped primarily by axion emission rather than gravitational waves. After axions acquire a mass at the QCD phase transition, they quickly become nonrelativistic and thus form a cold dark-matter component. Unknown initial conditions no longer enter, but details of the string mechanism are

sufficiently complicated to prevent an exact prediction of the axion density. On the basis of Battye & Shellard's treatment (406, 407), and assuming that axions are the cold dark matter of the universe, one finds a plausible mass range of $m_a = 6$–$2500\ \mu$eV (3). Sikivie et al (408–410) predict somewhat fewer axions, allowing for somewhat smaller masses if axions are the dark matter.

Either way, the ongoing full-scale search experiments for galactic dark-matter axions (Section 6.2.1 and Figure 13) in Livermore [US Axion Search (390)] and in Kyoto [CARRACK (391, 392)] aim at a cosmologically well-motivated range of axion masses (Figure 14).

7. LONG-RANGE FORCES

7.1 Fifth Force

New low-mass scalar or vector bosons would mediate long-range forces between macroscopic bodies. This is in contrast with pseudoscalars, which couple to the spin and thus produce no long-range force between unpolarized bodies except for a residual force from two-boson exchange (411–413). In stars, a new long-range force has two consequences. First, it modifies the effect of gravity. Second, it drains the star of energy, for the quanta of the new force are massless, or nearly so, and thus arise in thermal reactions.

Thermal graviton emission is a case in point (414–418). However, the graviton luminosity is very small, about $10^{-19}\,L_\odot$ for the Sun. Naturally, the coherent large-scale force is the most important aspect of gravity in stars. This conclusion carries over to new forces, notably a putative "fifth force."

According to experiment, a fifth force has to be much weaker than gravity (419–422), so that possible modifications of stellar structure (423, 424) or the solar p-mode frequencies (425, 426) are too small to be observable. Likewise, modifications of fundamental coupling constants near pulsars (427) or scalar boson emission by the Hulse-Taylor binary pulsar (428) are negligible effects.

However, there are no experimental fifth-force limits below about the centimeter scale, corresponding to boson masses exceeding about 10^{-3} eV, where the most restrictive bounds arise from the energy loss of stars. The Yukawa coupling g_S (g_V) of scalar (vector) bosons ϕ to electrons has been constrained by the bremsstrahlung process $e^- + {}^4\mathrm{He} \to {}^4\mathrm{He} + e^- + \phi$, which, with Equation 3, leads to $g_S \lesssim 1.3\times10^{-14}$ and $g_V \lesssim 0.9\times10^{-14}$ (4, 56, 57). The Yukawa coupling to baryons has been constrained by the Compton process $\gamma + {}^4\mathrm{He} \to {}^4\mathrm{He} + \phi$, leading to $g_S \lesssim 4.3\times10^{-11}$ and $g_V \lesssim 3.0\times10^{-11}$ (4, 56, 57).

7.2 Leptonic and Baryonic Gauge Interactions

It has been speculated that lepton and baryon numbers could play the role of gauge charges (429, 430). One consequence would be the existence of long-range leptonic and baryonic forces. The globular-cluster limits of the previous section

translate into limits of $e_L \lesssim 1\times10^{-14}$ and $e_B \lesssim 3\times10^{-11}$ on the leptonic and baryonic gauge charges. Tests of the equivalence principle on solar-system scales constrain a composition-dependent fifth force, leading to something like $e_{L,B} \lesssim 10^{-23}$ (431). The cosmic-background neutrinos would screen leptonic forces over large distances, but the solar-system limit on e_L would remain unaffected (113). On the other hand, the SN 1987A neutrino burst would not suffer dispersion in the leptonic field of the galaxy because it is shielded by the cosmic-background neutrinos (113). Leptonic forces contribute to the neutrino self-energy, modifying matter-induced neutrino oscillations in the Sun and supernovae (432, 433).

7.3 Time Variation of Newton's Constant

Astrophysics and cosmology are natural laboratories for testing all conceivable deviations from the standard theory of gravitation (434). One hypothesis, which goes back to Dirac's large-numbers hypothesis (435, 436), holds that the value of Newton's constant $G_{\rm N}$ evolves in time. The present-day rate of change can be measured by a precision study of the orbits of celestial bodies. In the solar system, data come from laser ranging of the Moon (437) and radar ranging of the planets, notably by the Viking landers on Mars (438). The increase of the length of day from 1663 to 1972 caused by tidal forces in the Earth-Moon system are consistent with a constant $G_{\rm N}$ (439), although some controversial claims for a decreasing $G_{\rm N}$ have been raised (434). Beginning in 1974, very precise orbital data exist for the Hulse-Taylor binary pulsar PSR 1923 + 16 (440). A weaker but less model-dependent bound arises from the spin-down rate of the pulsar PSR 0655 + 64 (441). Finally, the long-time stability of galaxy clusters limits a decreasing $G_{\rm N}$ (442). The bounds from these methods are summarized in Table 2.

TABLE 2 Range of allowed time variation of Newton's constant

Method	$\dot{G}_{\rm N}/G_{\rm N}$ $[10^{-12}\,{\rm yr}^{-1}]$ from	to	Authors	Year	Ref.
Laser ranging (Moon)	−8	8	Williams et al	1996	(437)
Radar ranging (Mars)	−12	8	Shapiro	1990	(438)
Length of day	−20	20	Morrison	1973	(439)
Binary Pulsar 1913 + 16	0	22	Damour & Taylor	1991	(440)
Spin-down PSR 0655 + 64	−55	55	Goldman	1990	(441)
Stability galaxy clusters	−60	—	Dearborn & Schramm	1974	(442)
Helioseismology	−2	2	Guenther et al	1998	(453)
Globular-cluster ages	−35	7	Degl'Innocenti et al	1996	(458)
Pulsar masses	−5	4	Thorsett	1996	(459)

Intriguing limits follow from the properties of the Sun. Paleontological evidence for its past luminosity, which scales approximately as $G_N^7 \mathcal{M}^5$, provides limits on previous values of G_N (443). Solar models with a time-varying G_N were studied in the 1960s and 1970 (444–450), but truly interesting limits arose only recently from helioseismological observations (451–453). Guenther et al derived a limit of $|\dot{G}_N/G_N| \lesssim 2 \times 10^{-12}$ yr^{-1} by comparing the measured small-spacing p-mode frequency differences with those calculated from solar models with a time-varying G_N (453). The authors believe that the uncertainty is dominated by the observational errors and that the prime systematic uncertainty is the exact solar age. A more conservative approach was used in deriving limits on a new solar energy-loss mechanism (Section 2.3). The helioseismological analysis of Guenther et al (453) provides the most restrictive limit on $\dot{G}_N/G_N$, which may stimulate other groups to reassess the bound independently.

A large effect is expected on the oldest stars, which "integrate" $G_N(t)$ into the distant past. White-dwarf cooling is a case in point (454, 455). Under reasonable assumptions for the galactic age, the faint end of the luminosity function prefers a negative value for $\dot{G}_N/G_N$, around -10 to -30×10^{-12} yr^{-1}. Very recently, this case has been reexamined in greater detail (456). The observational uncertainty of the faint end of the luminosity function and the uncertainty of the galactic age preclude a clear limit on $\dot{G}_N/G_N$. However, it is remarkable that even values as small as 10^{-14} yr^{-1} seem to make a noticeable difference to the cooling behavior of the oldest white dwarfs.

Globular clusters are another important case because a different G_N in the past changes their apparent age based on the brightness of the main-sequence turn-off (457–459). A comparison with the expansion age of the universe brackets the allowed rate of change to the interval shown in Table 2.

A very sensitive limit arises from the observed masses of several old pulsars, which measure the value of G_N at their time of formation in a SN explosion (460). The mass of a SN core at the time of collapse depends on its Chandrasekhar value, which in turn scales as ${G_N}^{-3/2}$.

The limits shown in Table 2 are difficult to compare on an equal footing because they involve vastly different ways of dealing with statistical and systematic uncertainties. However, it seems fair to conclude that $|\dot{G}_N/G_N|$ cannot exceed a few times 10^{-12} yr^{-1} and that stars play an important role in this discourse. A similar bound arises from the cosmic expansion rate at the time of big-bang nucleosynthesis as measured by the primordial light-element abundances (461). It implies that, three minutes after the big bang, G_N agreed with its present-day value to within a few tens of percent. A comparison of this limit with those of Table 2 requires a specific assumption about the functional dependence of $G_N(t)$.

7.4 Equivalence Principle

The general relativistic equivalence principle implies that the space-time trajectories of relativistic particles are independent of internal degrees of freedom, such as

spin or flavor, and independent of the particle type (e.g. photon, neutrino). Several astronomical observations allow tests of this prediction.

Limits on a gravitationally induced birefringence effect for photon propagation have been derived from the absence of depolarization of the Zeeman components of spectral lines emitted in magnetically active regions of the Sun (462). Observations of the light deflection by the Sun could soon become interesting (463). The depolarization effect on distant radio galaxies already provides very restrictive limits (464, 465), as do pulsar observations (466–468).

One may also test for the equality of the Shapiro time delay between different particles that propagate through the same gravitational field. The absence of an anomalous shift between the SN 1987A photon and neutrino arrival times (Section 4.2) gave limits on violations of the equivalence principle (116–118). The observation of a future galactic SN could provide independent arrival information for $\overline{\nu}_e$ and ν_e and thus provide another such test (108, 469).

A violation of the equivalence principle could manifest itself by a relative shift of the energies of different neutrino flavors in a gravitational field. For a given momentum p, the matrix of energies in flavor space (relativistic limit) is $E = p + M^2/2p + 2p\phi(\mathbf{r})(1 + F)$, where M^2 is the squared neutrino mass matrix, $\phi(\mathbf{r})$ is the Newtonian gravitational potential, and F is a matrix of dimensionless constants that parameterize the violation of the equivalence principle. $F \neq 0$ can lead to neutrino oscillations in analogy to the standard vacuum oscillations that are caused by the matrix M^2 (469–481). Values for F_{ij} in the general 10^{-14}–10^{-17} range could account for the solar neutrino problem.

7.5 Photon Mass

Although it is usually taken for granted that photons are strictly massless, this theoretical expectation still needs to be tested experimentally. Some of the most restrictive constraints are related to the long-range nature of static electric or magnetic fields. The best laboratory limit of $m_\gamma \lesssim 10^{-14}$ eV derives from a test of Coulomb's law (see (483) for a review).

In the astrophysical domain, the dispersion of the pulsed signal of radio pulsars is not a very sensitive diagnostic because the interstellar medium mimics a photon mass corresponding to a plasma frequency of order 10^{-11} eV. The spatial variation of magnetic fields of celestial bodies is far more sensitive. Jupiter's magnetic field, as measured by Pioneer-10, yields $m_\gamma \lesssim 0.6 \times 10^{-15}$ eV (484), and the Earth's field gives $m_\gamma \lesssim 0.8 \times 10^{-15}$ eV (485).

If the photon has a mass, Am_γ^2 is an observable quantity, where A is the vector potential corresponding to known magnetic fields. A recent laboratory experiment discloses $Am_\gamma^2 \lesssim 0.8 \times 10^{-22}$ T m eV^2 (486). The galactic magnetic field implies $A \approx 2 \times 10^9$ T m (Tesla-meter), so that $m_\gamma \lesssim 2 \times 10^{-16}$ eV, while a cluster-level field corresponds to $A \approx 10^{12}$ T m, providing $m_\gamma \lesssim 10^{-17}$ eV.

Even more restrictive limits obtain from astrophysical objects in which magnetic fields, and hence the Maxwellian form of electrodynamics, play a key role in

maintaining equilibrium or creating long-lived stable structures (487). The most restrictive case is based on an argument about the magneto-gravitational equilibrium of the gas in the Small Magellanic Cloud. The argument requires that the range of the interaction exceed the characteristic field scale of about 3 kpc (488). This resulting limit, $m_\gamma \lesssim 10^{-27}$ eV, if correct, is surprisingly close to 10^{-33} eV, where the photon Compton wavelength would exceed the radius of the observable universe and thus would cease to have any observable consequences.

7.6 Multibody Neutrino Exchange

Two-neutrino exchange between fermions gives rise to a long-range force. A neutrino may also pass around several fermions, so to speak, producing a much smaller potential. A thought-provoking paper has claimed that this multibody neutrino exchange could be a huge effect in neutron stars, essentially because combinatorial factors among many neutrons win out against the smallness of the potential (489). To stabilize neutron stars, it was claimed, the long-range nature of neutrino exchange had to be suppressed by a nonvanishing mass exceeding about 0.4eV for all flavors. An interesting series of papers has shown, however, that a proper resummation of a seemingly divergent series of terms leads to a well-behaved and small "neutron-star self-energy" (490–495), invalidating the claim of a lower neutrino mass limit.

8. CONCLUSION

Stellar-evolution theory, along with astronomical observations, the SN 1987A neutrino burst, and certain X- and γ-ray observations, provides a number of well-developed arguments to constrain the properties of low-mass particles. The most successful examples are globular-cluster stars, where the "energy-loss argument" was condensed into the simple criteria of Equations 2 and 3, and SN 1987A, where it was summarized by Equation 5. New particle-physics conjectures must pass these and other simple astrophysical standard tests before being taken seriously.

A showcase example for the interplay between astrophysical limits with laboratory experiments and cosmological arguments is provided by the axion hypothesis. The laboratory and astrophysical limits push the Peccei-Quinn scale to such high values that it appears almost inevitable that axions, if they exist at all, are important as a cold dark-matter component. This makes the direct search for galactic axion dark matter a well-motivated effort. Other important standard limits pertain to neutrino electromagnetic form factors. Laboratory experiments will have a difficult time catching up.

The globular-cluster limit was based on relatively old observational data. A plot like Figure 5 could be made more significant with dedicated CCD observations of globular clusters and improved theoretical interpretations. Assuming that such an effort produces internally consistent results, the statistical significance would improve, but I would not expect a vast gain for, say, the neutrino magnetic-moment limit, since there always remain irreducible systematic uncertainties.

Shockingly, SN 1987A as a particle-physics laboratory is based on no more than two dozen measured neutrinos. The observation of a future galactic SN with a large detector like Superkamiokande or a future observatory such as OMNIS (245) would provide a high-statistics neutrino "light" curve and thus a sound empirical basis for SN theory in general and for particle-physics interests in particular. Alas, galactic supernovae happen only once every few decades, perhaps only once per century. Thus, although the neutrinos from the next galactic SN surely are on their way, it could be a long wait until they arrive.

Most of the theoretical background relevant to this field could not be touched upon in this brief overview. The physics of weakly coupled particles in stars is a nice playing field for "particle physics in media," which involves field theory at finite temperature and density, many-body effects, particle dispersion and reactions in magnetic fields and media, oscillations of trapped neutrinos, and so forth. It is naturally in the context of SN theory that such issues are of particular interest, but even the plasmon decay $\gamma \to \nu\bar{\nu}$ in normal stars or the MSW effect in the Sun are interesting cases. Particle physics in media and its astrophysical and cosmological applications is a fascinating topic in its own right, which deserves a dedicated review.

Much more information of particle-physics interest may be written in the sky than has been deciphered as yet. Other objects or phenomena should be considered, perhaps other kinds of conventional stars, perhaps more exotic phenomena such as γ-ray bursts. The particle-physics lessons to be learned from them are left to be reviewed in a future report.

ACKNOWLEDGMENTS

This work was supported, in part, by the Deutsche Forschungsgemeinschaft under grant No. SFB-375.

LITERATURE CITED

1. Turner MS. *Phys. Rep.* 197:67 (1990)
2. Raffelt GG. *Phys. Rep.* 198:1 (1990)
3. Caso C, et al. *Eur. Phys. J.* C3:1 (1998)
4. Raffelt GG. *Stars as Laboratories for Fundamental Physics*. Chicago: Univ. Chicago Press (1996)
5. Bahcall J. *Neutrino Astrophysics*. Cambridge, UK: Cambridge Univ. Press (1989)
6. Castellani V, et al. *Phys. Rep.* 281:309 (1997)
7. Bahcall JN, Krastev PI, Smirnov AY. *Phys. Rev. D* 58:096016 (1998)

7a. Kayser B, et al. *Annu. Rev. Nucl. Part. Sci.* 49:481–527

8. Glendenning NK. *Compact Stars*. New York: Springer (1997)
9. Weber F. *Pulsars as Astrophysical Laboratories for Nuclear and Particle Physics*. Bristol, UK: Inst. Phys. (1999)
10. Alcock C, Olinto AV. *Annu. Rev. Nucl. Part. Sci.* 38:161 (1988)
11. Madsen J, Haensel P, eds. *Strange Quark Matter in Physics and Astrophysics, Nucl. Phys. (Proc. Suppl.)* 24B (1992)

12. Vassiliadis G, et al, eds. *Proc. Int. Symp. Strangeness and Quark Matter, Sept. 1–5, 1994, Crete, Greece*. Singapore: World Sci. (1995)
13. Kolb EW, Turner MS. *The Early Universe*. Reading, MA: Addison-Wesley (1990)
14. Freese K, Krasteva E. *Phys. Rev. D* 59: 063004 (1999).
15. Jungman G, Kamionkowski M, Griest K. *Phys. Rep.* 267:195 (1996)
16. Frieman JA, Dimopoulos S, Turner MS. *Phys. Rev. D* 36:2201 (1987)
17. Schlattl H, Weiss A, Raffelt G. *Astropart. Phys.* 10:353 (1999)
18. Raffelt G, Dearborn D. *Phys. Rev. D* 36: 2211 (1987)
19. Christensen-Dalsgaard J, Thompson DO, Gough DO. *Astrophys. J.* 378:413 (1991)
20. Degl'Innocenti S, Dziembowski WA, Fiorentini G, Ricci B. *Astropart. Phys.* 7:77 (1997)
21. Basu S, et al. *Mon. Not. R. Astr. Soc.* 292:243 (1997)
22. Carlson ED, Salati P. *Phys. Lett.* B218:79 (1989)
23. Raffelt G, Starkman G. *Phys. Rev. D* 40:942 (1989)
24. Buonanno R, et al. *Mem. Soc. Astron. Ital.* 57:391 (1986)
25. Renzini A, Fusi Pecci F. *Annu. Rev. Astron. Astrophys.* 26:199 (1988)
26. Clayton DD. *Principles of Stellar Evolution and Nucleosynthesis*. Chicago: Univ. Chicago Press (1968)
27. Kippenhahn R, Weigert A. *Stellar Structure and Evolution*. Berlin: Springer (1990)
28. Raffelt G. *Astrophys. J.* 365:559 (1990)
29. Castellani M, Degl'Innocenti S. *Astrophys. J.* 402:574 (1993)
30. Catelan M, de Freitas Pacheco JA, Horvath JE. *Astrophys. J.* 461:231 (1996)
31. Buzzoni A, et al. *Astron. Astrophys.* 128:94 (1983)
32. Raffelt G, Dearborn D. *Phys. Rev. D* 37:549 (1988)
33. Sutherland P, et al. *Phys. Rev. D* 13:2700 (1976)
34. Fukugita M, Yazaki S. *Phys. Rev. D* 36:3817 (1987)
35. Raffelt G, Dearborn D, Silk J. *Astrophys. J.* 336:64 (1989)
36. Raffelt GG. *Phys. Rev. Lett.* 64:2856 (1990)
37. Raffelt G, Weiss A. *Astron. Astrophys.* 264:536 (1992)
38. Dicus DA, et al. *Phys. Rev. D* 18:1829 (1978)
39. Mikaelian KO. *Phys. Rev. D* 18:3605 (1978)
40. Dicus DA, et al. *Phys. Rev. D* 22:839 (1980)
41. Georgi H, Glashow SL, Nussinov S. *Nucl. Phys.* B193:297 (1981)
42. Barroso A, Branco GC. *Phys. Lett.* B116:247 (1982)
43. Fukugita M, Watamura S, Yoshimura M. *Phys. Rev. Lett.* 48:1522 (1982)
44. Fukugita M, Watamura S, Yoshimura M. *Phys. Rev. D* 26:1840 (1982)
45. Krauss LM, Moody JE, Wilczek F. *Phys. Lett.* B144:391 (1984)
46. Brodsky SJ, et al. *Phys. Rev. Lett.* 56:1763 (1986)
47. Pantziris A, Kang K. *Phys. Rev. D* 33:3509 (1986)
48. Raffelt G. *Phys. Rev. D* 33:897 (1986)
49. Chanda R, Nieves JF, Pal PB. *Phys. Rev. D* 37:2714 (1988)
50. Raffelt G. *Phys. Rev. D* 41:1324 (1990)
51. Haxton WC, Lee KY. *Phys. Rev. Lett.* 66:2557 (1991)
52. Raffelt G, Weiss A. *Phys. Rev. D* 51:1495 (1995)
53. Hoffmann S. *Phys. Lett.* B193:117 (1987)
54. Raffelt G. *Phys. Rev. D* 38:3811 (1988)
55. van der Velde JC. *Phys. Rev. D* 39:1492 (1989)
56. Grifols JA, Massó E. *Phys. Lett.* B173:237 (1986)
57. Grifols JA, Massó E, Peris S. *Mod. Phys. Lett.* A4:311 (1989)
58. Bouquet A, Vayonakis CE. *Phys. Lett.* B116:219 (1982)
59. Fukugita M, Sakai N. *Phys. Lett.* B114:23 (1982)

60. Anand JD, et al. *Phys. Rev. D* 29:1270 (1984)
61. Sweigart AV, Gross PG. *Astrophys. J. Suppl.* 36:405 (1978)
62. Shapiro SL, Teukolsky SA. *Black Holes, White Dwarfs, and Neutron Stars*. New York: Wiley (1983)
63. Fleming TA, Liebert J, Green RF. *Astrophys. J.* 308:176 (1986)
64. Liebert J, Dahn CC, Monet DG. *Astrophys. J.* 332:891 (1988)
65. Koester D, Schönberner D. *Astron. Astrophys.* 154:125 (1986)
66. Mestel L. *Mon. Not. R. Astr. Soc.* 112:583 (1952)
67. Kepler SO, et al. *Astrophys. J.* 378:L45 (1991)
68. Kepler SO, et al. *Baltic Astron.* 4:221 (1995)
69. Raffelt G. *Phys. Lett.* B166:402 (1986)
70. Nakagawa M, Kohyama Y, Itoh N. *Astrophys. J.* 322:291 (1987)
71. Nakagawa M, et al. *Astrophys. J.* 326:241 (1988)
72. Wang J. *Mod. Phys. Lett.* A7:1497 (1992)
73. Blinnikov SI, Dunina-Barkovskaya NV. *Mon. Not. R. Astr. Soc.* 266:289 (1994)
74. Altherr T, Petitgirard E, del Río Gaztelurrutia T. *Astropart. Phys.* 2:175 (1994)
75. Isern J, Hernanz M, García-Berro E. *Astrophys. J.* 392:L23 (1992)
76. Tsuruta S. *Phys. Rep.* 292:1 (1998)
77. Iwamoto N. *Phys. Rev. Lett.* 53:1198 (1984)
78. Tsuruta S, Nomoto K. In *Observational Cosmology*, ed. A Hewitt, et al. IAU Symp. No. 124 (1987)
79. Umeda H, et al. In *Proc. Neutron Stars and Pulsars, 17–20 Nov. 1997, Tokyo, Japan*, ed. N Shibazaki, et al. Singapore: World Sci. (1998)
80. Iwamoto N, et al. *Phys. Rev. D* 51:348 (1995)
81. Umeda H, Nomoto K, Tsuruta S. *Astrophys. J.* 431:309 (1994)
82. Umeda H, Tsuruta S, Nomoto K. *Astrophys. J.* 433:256 (1994)
83. Suy IS, Lee CH. *Phys. Lett.* B 432:145 (1998)
84. Schramm DN, Truran JW. *Phys. Rep.* 189:89 (1990)
85. Raffelt GG. *Mod. Phys. Lett.* A5:2581 (1990)
86. Koshiba M. *Phys. Rep.* 220:229 (1992)
87. Brown GE, Bethe HA, Baym G. *Nucl. Phys.* A375:481 (1982)
88. Bethe HA. *Rev. Mod. Phys.* 62:801 (1990)
89. Petschek AG, ed. *Supernovae*. New York: Springer (1990)
90. Cooperstein J. *Phys. Rep.* 163:95 (1988)
91. Burrows A. *Annu. Rev. Nucl. Part. Sci.* 40:181 (1990)
92. Janka HT. In *Proc. Volcano Workshop 1992: Frontier Objects in Astrophysics and Particle Physics*, ed. F Giovannelli, G Mannocchi. *Conf. Proc. Soc. Ital. Fis.* Vol. 40 (1993)
93. Hirata KS, et al. *Phys. Rev. D* 38:448 (1988)
94. Bratton CB, et al. *Phys. Rev. D* 37:3361 (1988)
95. Alexeyev EN, et al. *Pis'ma Zh. Eksp. Teor. Fiz.* 45:461 (1987) [*JETP Lett*. 45:589 (1987)]
96. Loredo TJ, Lamb DQ. In *Proc. 14th Texas Symp. Relativistic Astrophysics*, ed. EJ Fenyves. *Ann. NY Acad. Sci.* 571:601 (1989)
97. Loredo TJ. *From Laplace to Supernova SN 1987A: Bayesian Inference in Astrophysics*. PhD thesis, Univ. Chicago (1995)
98. Janka HT, Hillebrandt W. *Astron. Astrophys.* 224:49 (1989)
99. Jegerlehner B, Neubig F, Raffelt G. *Phys. Rev. D* 54:1194 (1996)
100. Lattimer JM, Yahil A. *Astrophys. J.* 340:426 (1989)
101. LoSecco JM. *Phys. Rev. D* 39:1013 (1989)
102. Kielczewska D. *Phys. Rev. D* 41:2967 (1990)
103. Zatsepin GI. *Pis'ma Zh. Eksp. Teor. Fiz.* 8:333 (1968) [*JETP Lett*. 8:205 (1968)]
104. Kernan PJ, Krauss LM. *Nucl. Phys.* B437:243 (1995)

105. Barbiellini G, Cocconi G. *Nature* 329:21 (1987)
106. Fujiwara K. *Phys. Rev. D* 39:1764 (1989)
107. Atzmon E, Nussinov S. *Phys. Lett.* B328: 103 (1994)
108. Pakvasa S, Simmons WA, Weiler TJ. *Phys. Rev. D* 39:1761 (1989)
109. Grifols JA, Massó E, Peris S. *Phys. Lett.* B207:493 (1988)
110. Grifols JA, Massó E, Peris S. *Astropart. Phys.* 2:161 (1994)
111. Fiorentini G, Mezzorani G. *Phys. Lett.* B221:353 (1989)
112. Malaney RA, Starkman GD, Tremaine S. *Phys. Rev. D* 51:324 (1995)
113. Dolgov AD, Raffelt GG. *Phys. Rev. D* 52:2581 (1995)
114. Longo MJ. *Phys. Rev. D* 36:3276 (1987)
115. Stodolsky L. *Phys. Lett.* B201:353 (1988)
116. Krauss LM, Tremaine S. *Phys. Rev. Lett.* 60:176 (1988)
117. Coley AA, Tremaine S. *Phys. Rev. D* 38:2927 (1988)
118. Almeida LD, Matsas GEA, Natale AA. *Phys. Rev. D* 39:677 (1989)
119. Ellis J, Olive KA. *Phys. Lett.* B193:525 (1987)
120. Raffelt G, Seckel D. *Phys. Rev. Lett.* 60: 1793 (1988)
121. Turner MS. *Phys. Rev. Lett.* 60:1797 (1988)
122. Mayle R, et al. *Phys. Lett.* B203:188 (1988)
123. Mayle R, et al. *Phys. Lett.* B219:515 (1989)
124. Burrows A, Turner MS, Brinkmann RP. *Phys. Rev. D* 39:1020 (1989)
125. Burrows A, Ressell T, Turner MS. *Phys. Rev. D* 42:3297 (1990)
126. Janka HT, Keil W, Raffelt G, Seckel D. *Phys. Rev. Lett.* 76:2621 (1996)
127. Keil W, et al. *Phys. Rev. D* 56:2419 (1997)
128. Grifols JA, Massó E, Peris S. *Phys. Lett.* B215:593 (1988)
129. Aharonov Y, Avignone FT III, Nussinov S. *Phys. Rev. D* 37:1360 (1988)
130. Aharonov Y, Avignone FT III, Nussinov S. *Phys. Lett.* B200:122 (1988)
131. Aharonov Y, Avignone FT III, Nussinov S. *Phys. Rev. D* 39:985 (1989)
132. Choi K, Kim CW, Kim J, Lam WP. *Phys. Rev. D* 37:3225 (1988)
133. Choi K, Santamaria A. *Phys. Rev. D* 42: 293 (1990)
134. Chang S, Choi K. *Phys. Rev. D* 49:12 (1994)
135. Ellis J, et al. *Phys. Lett.* B215:404 (1988)
136. Lau K. *Phys. Rev. D* 47:1087 (1993)
137. Nowakowski M, Rindani SD. *Phys. Lett.* B348:115 (1995)
138. Grifols JA, Massó E, Peris S. *Phys. Lett.* B220:591 (1989)
139. Grifols JA, Mohapatra RN, Riotto A. *Phys. Lett.* B400:124 (1997)
140. Grifols JA, Mohapatra RN, Riotto A. *Phys. Lett.* B401:283 (1997)
141. Grifols JA, Massó E, Toldra R. *Phys. Rev. D* 57:614 (1998)
142. Dicus DA, Mohapatra RN, Teplitz VL. *Phys. Rev. D* 57:578 (1998); (E) 57:4496 (1998)
143. Arkani-Hamed N, Dimopoulos S, Dvali G. *Phys. Rev. D* 59:086004 (1999)
144. Cullen S, Perelstein M. hep-ph/9903422 (1999)
145. Gaemers KJF, Gandhi R, Lattimer JM. *Phys. Rev. D* 40:309 (1989)
146. Grifols JA, Massó E. *Phys. Lett.* B242:77 (1990)
147. Gandhi R, Burrows A. *Phys. Lett.* B246: 149 (1990); (E) 261:519 (1991)
148. Mayle R, et al. *Phys. Lett.* B317:119 (1993)
149. Maalampi J, Peltoniemi JT. *Phys. Lett.* B269:357 (1991)
150. Turner MS. *Phys. Rev. D* 45:1066 (1992)
151. Pantaleone J. *Phys. Rev. D* 46:510 (1992)
152. Burrows A, Gandhi R, Turner MS. *Phys. Rev. Lett.* 68:3834 (1992)
153. Goyal A, Dutta S. *Phys. Rev. D* 49:3910 (1994)
154. Babu KS, Mohapatra RN, Rothstein IZ. *Phys. Rev. D* 45:5 (1992)

155. Babu KS, Mohapatra RN, Rothstein IZ. *Phys. Rev. D* 45:3312 (1992)
156. Kainulainen K, Maalampi J, Peltoniemi JT. *Nucl. Phys.* B358:435 (1991)
157. Raffelt G, Sigl G. *Astropart. Phys.* 1:165 (1993)
158. Barbieri R, Mohapatra RN. *Phys. Rev. D* 39:1229 (1989)
159. Grifols JA, Massó E. *Nucl. Phys.* B331:244 (1990)
160. Grifols JA, Massó E, Rizzo TG. *Phys. Rev. D* 42:3293 (1990)
161. Rizzo TG. *Phys. Rev. D* 44:202 (1991)
162. Lattimer JM, Cooperstein J. *Phys. Rev. Lett.* 61:23 (1988)
163. Barbieri R, Mohapatra RN. *Phys. Rev. Lett.* 61:27 (1988)
164. Goyal A, Dutta S. *Phys. Rev. D* 49:5593 (1994)
165. Goyal A, Dutta S, Choudhury SR. *Phys. Lett.* B346:312 (1995)
166. Ayala A, D'Olivo JC, Torres M. hep-ph/9804230 (1998)
167. Mohapatra RN, Rothstein IZ. *Phys. Lett.* B247:593 (1990)
168. Grifols JA, Massó E. *Phys. Rev. D* 40:3819 (1989)
169. Engel J, Seckel D, Hayes AC. *Phys. Rev. Lett.* 65:960 (1990)
170. Dodelson S, Frieman JA, Turner MS. *Phys. Rev. Lett.* 68:2572 (1992)
171. Chupp EL, Vestrand WT, Reppin C. *Phys. Rev. Lett.* 62:505 (1989)
172. Oberauer L, et al. *Astropart. Phys.* 1:377 (1993)
173. von Feilitzsch F, Oberauer L. *Phys. Lett.* B200:580 (1988)
174. Kolb EW, Turner MS. *Phys. Rev. Lett.* 62:509 (1989)
175. Bludman SA. *Phys. Rev. D* 45:4720 (1992)
176. Jaffe AH, Turner MS. *Phys. Rev. D* 55: 7951 (1997)
177. Miller RS. *A Search for Radiative Neutrino Decay and its Potential Contribution to the Cosmic Diffuse Gamma-Ray Flux*. PhD thesis, Univ. New Hampshire (1995)
178. Miller RS, Ryan JM, Svoboda RC. *Astron. Astrophys. Suppl. Ser.* 120:635 (1996)
179. Dar A, Dado S. *Phys. Rev. Lett.* 59:2368 (1987)
180. Mohapatra RN, Nussinov S, Zhang X. *Phys. Rev. D* 49:3434 (1994)
181. Schmid H, Raffelt G, Leike A. *Phys. Rev. D* 58:113004 (1998)
182. Dar A, Goodman J, Nussinov S. *Phys. Rev. Lett.* 58:2146 (1987)
183. Nussinov S, Rephaeli Y. *Phys. Rev. D* 36: 2278 (1987)
184. Goldman I, et al. *Phys. Rev. Lett.* 60:1789 (1988)
185. Voloshin MB. *Phys. Lett.* B209:360 (1988)
186. Okun LB. *Yad. Fiz.* 48:1519 (1988) [*Sov. J. Nucl. Phys*. 48:967 (1988)]
187. Blinnikov SI, Okun LB. *Pis'ma Astron. Zh.* 14:867 (1988) [*Sov. Astron. Lett*. 14: 368 (1988)]
188. Falk SW, Schramm DN. *Phys. Lett.* B79: 511 (1978)
189. Takahara M, Sato K. *Phys. Lett.* B174:373 (1986)
190. Mikheyev SP, Smirnov AY. *Zh. Eksp. Teor. Fiz.* 91:7 (1986) [*Sov. Phys. JETP* 64:4 (1986)]
191. Arafune J, et al. *Phys. Rev. Lett.* 59:1864 (1987)
192. Arafune J, et al. *Phys. Lett.* B194:477 (1987)
193. Lagage PO, et al. *Phys. Lett.* B193:127 (1987)
194. Minakata H, et al. *Mod. Phys. Lett.* A2:827 (1987)
195. Nötzold D. *Phys. Lett.* B196:315 (1987)
196. Walker TP, Schramm DN. *Phys. Lett.* B195:331 (1987)
197. Kuo TK, Pantaleone J. *Phys. Rev. D* 37:298 (1988)
198. Minakata H, Nunokawa H. *Phys. Rev. D* 38:3605 (1988)
199. Rosen SP. *Phys. Rev. D* 37:1682 (1988)

200. Fuller GM, et al. *Astrophys. J.* 389:517 (1992)
201. Janka HT, Hillebrandt W. *Astron. Astrophys. Suppl.* 78:375 (1989)
202. Janka HT. *Astropart. Phys.* 3:377 (1995)
203. Suzuki H. *Num. Astrophys. Jpn.* 2:267 (1991)
204. Suzuki H. In *Frontiers of Neutrino Astrophysics, Proc. Int. Symp. Neutrino Astrophysics*, 19–22 Oct. 1992, *Takayama/Kamioka, Japan*, ed. Y Suzuki, K Nakamura. Tokyo: Universal Acad. Press (1993)
205. Hannestad S, Raffelt G. *Astrophys. J.* 507:339 (1998)
206. Woosley SE, Hoffmann RD. *Astrophys. J.* 395:202 (1992)
207. Meyer BS, et al. *Astrophys. J.* 399:656 (1992)
208. Witti J, Janka HT, Takahashi K. *Astron. Astrophys.* 286:841 (1994)
209. Takahashi K, Witti J, Janka HT. *Astron. Astrophys.* 286:857 (1994)
210. Meyer BS. *Annu. Rev. Astron. Astrophys.* 32:153 (1994)
211. Meyer BS. *Astrophys. J.* 449:L55 (1995)
212. Meyer BS, McLaughlin GC, Fuller GM. *Phys. Rev.* C58:3696 (1998)
213. Qian YZ, et al. *Phys. Rev. Lett.* 71:1965 (1993)
214. Qian YZ, Fuller GM. *Phys. Rev. D* 51:1479 (1995)
215. Sigl G. *Phys. Rev. D* 51:4035 (1995)
216. Pantaleone J. *Phys. Lett.* B342:250 (1995)
217. Laughlin GC, et al. astro-ph/9902106 (1999)
218. Kusenko A, Segrè G. *Phys. Rev. Lett.* 77:4872 (1996)
219. Qian YZ. *Phys. Rev. Lett.* 79:2750 (1997)
220. Kusenko A, Segrè G. *Phys. Rev. Lett.* 79:2751 (1997)
221. Kusenko A, Segrè G. *Phys. Lett.* B396: 197 (1997)
222. Akhmedov EK, Lanza A, Sciama DW. *Phys. Rev. D* 56:6117 (1997)
223. Grasso D, Nunokawa H, Valle JWF. *Phys. Rev. Lett.* 81:2412 (1998)
224. Horvat R. *Mod. Phys. Lett.* A13:2379 (1998)
225. Kusenko A, Segrè G. *Phys. Rev. D* 59:061302 (1999)
226. Janka HT, Raffelt GG. *Phys. Rev. D* 59:023005 (1999)
227. Smirnov AY, Spergel DN, Bahcall JN. *Phys. Rev. D* 49:1389 (1994)
228. Valle JWF. In *Proc. New Trends in Neutrino Physics, Tegernsee, Ringberg Castle, Germany, 24–29 May 1998*. In press. hep-ph/9809234 (1998)
229. Kayser B. In *Proc. Int. Conf. High-Energy Physics (ICHEP 98), 29th, Vancouver, Canada, 23–29 July 1998*. In press. hep-ph/9810513 (1998)
230. Smirnov A. *Proc. Int. WEIN Symp., 5th: Conf. on Physics Beyond the Standard Model (WEIN 98), Santa Fe, New Mexico, 14–21 June 1998*. In press. hep-ph/9901208 (1999)
231. Fukuda Y, et al (Superkamiokande Collaboration). *Phys. Rev. Lett.* 81:1562 (1998)
232. Athanassopoulos C, et al. *Phys. Rev. Lett.* 77:3082 (1996)
233. Athanassopoulos C, et al. *Phys. Rev. Lett.* 81:1774 (1998)
234. Nunokawa H, Peltoniemi JT, Rossi A, Valle JWF. *Phys. Rev. D* 56:1704 (1997)
235. Qian YZ, Fuller GM. *Phys. Rev. D* 49:1762 (1994)
236. Choubey S, Majumdar D, Kar K. *J. Phys.* G25:1001 (1999)
237. Fuller GM, Haxton WC, McLaughlin GC. *Phys. Rev. D* 59:085005 (1999)
238. Totani T. *Phys. Rev. Lett.* 80:2039 (1998)
239. Seckel D, Steigman G, Walker T. *Nucl. Phys.* B366:233 (1991)
240. Krauss LM, et al. *Nucl. Phys.* B380:507 (1992)
241. Fiorentini G, Acerbi C. *Astropart. Phys.* 7:245 (1997)
242. Beacom JF, Vogel P. *Phys. Rev. D* 58: 093012 (1998)

243. Beacom JF, Vogel P. *Phys. Rev. D* 58: 053010 (1998)
244. Cline D, et al. *Phys. Rev. D* 50:720 (1994)
245. Smith PF. *Astropart. Phys.* 8:27 (1997)
246. Morrison DRO. *Nature* 366:29 (1993)
247. Mohapatra RN, Pal P. *Massive Neutrinos in Physics and Astrophysics*. Singapore: World Sci. (1991)
248. Winter K, ed. *Neutrino Physics.* Cambridge, UK: Cambridge Univ. Press (1991)
249. Lucio JL, Rosado A, Zepeda A. *Phys. Rev. D* 31:1091 (1985)
250. Auriemma G, Srivastava Y, Widom A. *Phys. Lett.* B195:254 (1987)
251. Degrassi G, Sirlin A, Marciano WJ. *Phys. Rev. D* 39:287 (1989)
252. Musolf MJ, Holstein BR. *Phys. Rev. D* 43:2956 (1991)
253. Góngora A, Stuart RG. *Z. Phys. C* 55:101 (1992)
254. Salati P. *Astropart. Phys.* 2:269 (1994)
255. D'Olivo JC, Nieves JF, Pal PB. *Phys. Rev. D* 40:3679 (1989)
256. Altherr T, Salati P. *Nucl. Phys.* B421:662 (1994)
257. Adams JB, Ruderman MA, Woo CH. *Phys. Rev.* 129:1383 (1963)
258. Zaidi MH. *Nuovo Cim.* 40:502 (1965)
259. Haft M, Raffelt G, Weiss A. *Astrophys. J.* 425:222 (1994); (E) *Astrophys. J*. 438: 1017 (1995)
260. Bernstein J, Ruderman MA, Feinberg G. *Phys. Rev.* 132:1227 (1963)
261. Broggini C, et al (MUNU Collaboration). *Nucl. Phys. (Proc. Suppl.)* B70:188 (1999)
262. Oberauer L, von Feilitzsch F, Mössbauer RL. *Phys. Lett.* B198:113 (1987)
263. Cowsik R. *Phys. Rev. Lett.* 39:784 (1977)
264. Raffelt G. *Phys. Rev. D* 31:3002 (1985)
265. Ressell MT, Turner MS. *Comments Astrophys.* 14:323 (1990)
266. Biller SD, et al. *Phys. Rev. Lett.* 80:2992 (1998)
267. Raffelt GG. *Phys. Rev. Lett.* 81:4020 (1998)
268. Henry RC, Feldmann PD. *Phys. Rev. Lett.* 47:618 (1981)
269. Davidsen AF, et al. *Nature* 351:128 (1991)
270. Ioannissyan A, Raffelt G. *Phys. Rev. D* 55:7038 (1997)
271. Elmfors P, Enqvist K, Raffelt G, Sigl G. *Nucl. Phys.* B503:3 (1997)
272. Fujikawa K, Shrock R. *Phys. Rev. Lett.* 45:963 (1980)
273. Okun LB. *Yad. Fiz.* 44:847 (1986) [*Sov. J. Nucl. Phys*. 44:546 (1986)]
274. Werntz CW. Unpublished (1970), as quoted in Ref. 275
275. Cisneros A. *Astrophys. Space Sci.* 10:87 (1971)
276. Voloshin MB, Vysotskiĭ MI. *Yad. Fiz.* 44:845 (1986) [*Sov. J. Nucl. Phys*. 44:544 (1986)]
277. Nötzold D. *Phys. Rev. D* 38:1658 (1988)
278. Schechter J, Valle JWF. *Phys. Rev. D* 24:1883 (1981); (E) 25:283 (1982)
279. Voloshin MB, Vysotskiĭ MI, Okun LB. *Yad. Fiz.* 44:677 (1986) [*Sov. J. Nucl. Phys*. 44:440 (1986)]
280. Voloshin MB, Vysotskiĭ MI, Okun LB. *Zh. Eksp. Teor. Fiz.* 91:754 (1986); (E) 92:368 (1987) [*Sov. Phys. JETP* 64:446; (E) 65:209 (1987)]
281. Akhmedov EK. *Yad. Fiz.* 48:599 (1988) [*Sov. J. Nucl. Phys*. 48:382 (1988)]
282. Akhmedov EK. *Phys. Lett.* B213:64 (1988)
283. Barbieri R, Fiorentini G. *Nucl. Phys.* B304:909 (1988)
284. Lim CS, Marciano WJ. *Phys. Rev. D* 37:1368 (1988)
285. Akhmedov EK, Lanza A, Petcov ST. *Phys. Lett.* B348:124 (1995)
286. Guzzo MM, Nunokawa H. hep-ph/9810408 (1998)
287. Barbieri R, et al. *Phys. Lett.* B259:119 (1991)
288. Fiorentini G, Moretti M, Villante FL. *Phys. Lett.* B413:378 (1997)
289. Pastor S, Semikoz VB, Valle JWF. *Phys. Lett.* B423:118 (1998)

290. Athar H, Peltoniemi JT, Smirnov AY. *Phys. Rev. D* 51:6647 (1995)
291. Totani T, Sato K. *Phys. Rev. D* 54:5975 (1996)
292. Akhmedov EK, Lanza A, Petcov ST, Sciama DW. *Phys. Rev. D* 55:515 (1997)
293. Brüggen M. *Phys. Rev. D* 55:5876 (1997)
294. Nunokawa H, Qian YZ, Fuller GM. *Phys. Rev. D* 55:3265 (1997)
295. Babu KS, Mohapatra RN. *Phys. Rev. D* 42:3866 (1990)
296. Maruno M, Takasugi E, Tanaka M. *Prog. Theor. Phys.* 86:907 (1991)
297. Takasugi E, Tanaka M. *Prog. Theor. Phys.* 87:679 (1992)
298. Babu KS, Mohapatra RN, Rothstein IZ. *Phys. Rev. D* 45:R3312 (1992)
299. Foot R, Lew H, Volkas RR. *J. Phys. G: Nucl. Part. Phys.* 19:361 (1993); (E) 19:1067 (1993)
300. Holdom B. *Phys. Lett.* B166:196 (1986)
301. Dobroliubov MI, Ignatiev AY. *Phys. Rev. Lett.* 65:679 (1990)
302. Davidson S, Campbell B, Bailey D. *Phys. Rev. D* 43:2314 (1991)
303. Babu KS, Volkas RR. *Phys. Rev. D* 46:R2764 (1992)
304. Mohapatra RN, Nussinov S. *Int. J. Mod. Phys.* A7:3817 (1992)
305. Davidson S, Peskin M. *Phys. Rev. D* 49:2114 (1994)
306. Baumann J, et al. *Phys. Rev. D* 37:3107 (1988)
307. Marinelli M, Morpurgo G. *Phys. Lett.* B137:439 (1984)
308. Prinz AA, et al. *Phys. Rev. Lett.* 81:1175 (1998)
309. Jodidio A, et al. *Phys. Rev. D* 34:1967 (1986); (E) 37:237 (1988)
310. Ellis J, Enqvist K, Nanopoulos DV, Sarkar S. *Phys. Lett.* B167:457 (1986)
311. Gelmini GB, Roncadelli M. *Phys. Lett.* B99:411 (1981)
312. Chicashige Y, Mohapatra RN, Peccei RD. *Phys. Lett.* B98:265 (1981)
313. Berezhiani ZG, Smirnov AY, Valle JWF. *Phys. Lett.* B291:99 (1992)
314. Kikuchi H, Ma E. *Phys. Lett.* B335:444 (1994)
315. Kolb EW, Turner MS. *Phys. Rev. D* 36:2895 (1987)
316. Kolb EW, Tubbs DL, Dicus DA. *Astrophys. J.* 255:L57 (1982)
317. Dicus DA, Kolb EW, Tubbs DL. *Nucl. Phys.* B223:532 (1983)
318. Manohar A. *Phys. Lett.* B192:217 (1987)
319. Konoplich RV, Khlopov MY. *Yad. Fiz.* 47:891 (1988) [*Sov. J. Nucl. Phys.* 47:565 (1988)]
320. Fuller GM, Mayle R, Wilson JR. *Astrophys. J.* 332:826 (1988)
321. Berezhiani ZG, Smirnov AY. *Phys. Lett.* B220:279 (1989)
322. Valle JWF. *Phys. Lett.* B199:432 (1987)
323. Langacker P, London D. *Phys. Rev. D* 38:907 (1988)
324. Guzzo MM, Masiero A, Petcov ST. *Phys. Lett.* B260:154 (1991)
325. Roulet E. *Phys. Rev. D* 44:935 (1991)
326. Barger V, Phillips RJN, Whisnant K. *Phys. Rev. D* 44:1629 (1991)
327. Bergmann S. *Nucl. Phys.* B515:363 (1998)
328. Nunokawa H, Qian YZ, Rossi A, Valle JWF. *Phys. Rev. D* 54:4356 (1996)
329. Bergmann S, Kagan A. *Nucl. Phys.* B538:368 (1999)
330. Peccei RD, Quinn HR. *Phys. Rev. Lett.* 38:1440 (1977)
331. Peccei RD, Quinn HR. *Phys. Rev. D* 16:1791 (1977)
332. Weinberg S. *Phys. Rev. Lett.* 40:223 (1978)
333. Wilczek F. *Phys. Rev. Lett.* 40:279 (1978)
334. Kim JE. *Phys. Rep.* 150:1 (1987)
335. Cheng HY. *Phys. Rep.* 158:1 (1988)
336. Sikivie P. *Proc. Axion Workshop, University of Florida, Gainesville, Florida, USA, 13–15 March 1998*, in *Nucl. Phys. B (Proc. Suppl.)* In press (1999)
337. Carena M, Peccei RD. *Phys. Rev. D* 40:652 (1989)
338. Choi K, Kang K, Kim JE. *Phys. Rev. Lett.* 62:849 (1989)

339. Turner MS, Kang HS, Steigman G. *Phys. Rev. D* 40:299 (1989)
340. Iwamoto N. *Phys. Rev. D* 39:2120 (1989)
341. Dine M, Fischler W, Srednicki M. *Phys. Lett.* B104:199 (1981)
342. Zhitnitskiĭ AP. *Yad. Fiz.* 31:497 (1980) [*Sov. J. Nucl. Phys*. 31:260 (1980)]
343. Kim JE. *Phys. Rev. Lett.* 43:103 (1979)
344. Shifman MA, Vainshtein AI, Zakharov VI. *Nucl. Phys.* B166:493 (1980)
345. Kaplan DB. *Nucl. Phys.* B260:215 (1985)
346. Cheng SL, Geng CQ, Ni WT. *Phys. Rev. D* 52:3132 (1995)
347. Kim JE. *Phys. Rev. D* 58:055006 (1998)
348. Raffelt G. *Phys. Rev. D* 37:1356 (1988)
349. Massó E, Toldrà R. *Phys. Rev. D* 52:1755 (1995)
350. Massó E, Toldrà R. *Phys. Rev. D* 55:7967 (1997)
351. Cameron R, et al. *Phys. Rev. D* 47:3707 (1993)
352. Mori F. *Mod. Phys. Lett.* A11:715 (1996)
353. Sikivie P. *Phys. Rev. Lett.* 51:1415 (1983); (E) 52:695 (1984)
354. van Bibber K, Morris D, McIntyre P, Raffelt G. *Phys. Rev. D* 39:2089 (1989)
355. Lazarus DM, et al. *Phys. Rev. Lett.* 69: 2333 (1992)
356. Moriyama S, et al. *Phys. Lett.* B434:147 (1998)
357. Moriyama S. *Direct Search for Solar Axions by Using Strong Magnetic Field and X-Ray Detectors*. PhD thesis (in English), Univ. Tokyo (1998)
358. Raffelt G, Stodolsky L. *Phys. Rev. D* 37:1237 (1988)
359. Vorob'ev PV, Kolokolov IV. astroph/ 9501042 (1995)
360. Zioutas K, et al. *Nucl. Instrum. Methods* A425:482 (1999)
361. Buchmüller W, Hoogeveen F. *Phys. Lett.* B237:278 (1990)
362. Paschos EA, Zioutas K. *Phys. Lett.* B323:367 (1994)
363. Creswick RJ, et al. *Phys. Lett.* B427:235 (1998)
364. Avignone III FT, et al (SOLAX Collaboration). *Phys. Rev. Lett.* 81:5068 (1998)
365. Cebrián S, et al. *Astropart. Phys.* 10:397 (1999)
366. Carlson ED, Tseng LS. *Phys. Lett.* B365: 193 (1996)
367. Carlson ED. *Phys. Lett.* B344:245 (1995)
368. Brockway JW, Carlson ED, Raffelt GG. *Phys. Lett.* B383:439 (1996)
369. Gifols JA, Massó E, Toldrà R. *Phys. Rev. Lett.* 77:2372 (1996)
370. Krasnikov SV. *Phys. Rev. Lett.* 76:2633 (1996)
371. Morris DE. *Phys. Rev. D* 34:843 (1986)
372. Yoshimura M. *Phys. Rev. D* 37:2039 (1988)
373. Yanagida T, Yoshimura M. *Phys. Lett.* B202:301 (1988)
374. Gnedin YN, Krasnikov SV. *Zh. Eksp. Teor. Fiz.* 102:1729 (1992) [*Sov. Phys. JETP* 75:933 (1992)]
375. Gnedin YN, Krasnikov SV. *Astron. Lett.* 20:72 (1994)
376. Gnedin YN. *Comments Astrophys.* 18: 257 (1996)
377. Gnedin YN. *Astrophys. Space Sci.* 249: 125 (1997)
378. Carlson ED, Garretson WD. *Phys. Lett.* B336:431 (1994)
379. Mohanty S, Nayak SN. *Phys. Rev. Lett.* 70:4038 (1993); (E) 71:1117 (1993); (E) 76:2825 (1996)
380. Maiani L, Petronzio R, Zavattini E. *Phys. Lett.* B175:359 (1986)
381. Semertzidis Y, et al. *Phys. Rev. Lett.* 64:2988 (1990)
382. Bakalov D, et al. *Quantum Semiclass. Opt.* 10:239 (1998)
383. Lee S, et al. *Fermilab Proposal E-877* (1995)
384. Ruoso G, et al. *Z. Phys. C* 56:505 (1992)
385. Bershady MA, Ressel MT, Turner MS. *Phys. Rev. Lett.* 66:1398 (1991)
386. Ressell MT. *Phys. Rev. D* 44:3001 (1991)
387. Overduin JM, Wesson PS. *Astrophys. J.* 414:449 (1993)
388. Wuensch WU, et al. *Phys. Rev. D* 40:3153 (1989)

389. Hagmann C, et al. *Phys. Rev. D* 42:1297 (1990)
390. Hagmann C, et al. *Phys. Rev. Lett.* 80: 2043 (1998)
391. Ogawa I, Matsuki S, Yamamoto K. *Phys. Rev. D* 53:R1740 (1996)
392. Yamamoto K, Matsuki S. In *Proc. Int. Workshop Identification of Dark Matter (IDM 98), 2nd, Buxton, England, 7–11 Sept. 1998*. In press. hep-ph/9811487 (1998)
393. Moroi T, Murayama H. *Phys. Lett.* B440: 69 (1998)
394. Moriyama S. *Phys. Rev. Lett.* 75:3222 (1995)
395. Krčmar M, et al. *Phys. Lett.* B442:38 (1998)
396. Preskill J, Wise M, Wilczek F. *Phys. Lett.* B120:127 (1983)
397. Abbott L, Sikivie P. *Phys. Lett.* B120:133 (1983)
398. Dine M, Fischler W. *Phys. Lett.* B120:137 (1983)
399. Turner MS. *Phys. Rev. D* 33:889 (1986)
400. Lyth DH. *Phys. Lett.* B236:408 (1990)
401. Turner MS, Wilczek F. *Phys. Rev. Lett.* 66:5 (1991)
402. Linde A. *Phys. Lett.* B259:38 (1991)
403. Shellard EPS, Battye RA. astro-ph/ 9802216 (1998)
404. Davis RL. *Phys. Lett.* B180:225 (1986)
405. Davis RL, Shellard EPS. *Nucl. Phys.* B324:167 (1989)
406. Battye RA, Shellard EPS. *Nucl. Phys.* B423:260 (1994)
407. Battye RA, Shellard EPS. *Phys. Rev. Lett.* 73:2954 (1994); (E) 76:2203 (1996)
408. Harari D, Sikivie P. *Phys. Lett.* B195:361 (1987)
409. Hagmann C, Sikivie P. *Nucl. Phys.* B363:247 (1991)
410. Chang S, Hagmann C, Sikivie P. *Phys. Rev. D* 59:023505 (1999)
411. Grifols JA, Tortosa S. *Phys. Lett.* B328:98 (1994)
412. Ferrer F, Grifols JA. *Phys. Rev. D* 58: 096006 (1998)
413. Ferrer F, Nowakowski M. *Phys. Rev. D* 59:075009 (1999)
414. Papini G, Valluri SR. *Phys. Rep.* 33:51 (1977)
415. Papini G, Valluri SR. *Astron. Astrophys.* 208:345 (1989)
416. Schäfer G, Dehnen H. *Phys. Rev. D* 27:2864 (1983)
417. Gould RJ. *Astrophys. J.* 288:789 (1985)
418. del Campo S, Ford LH. *Phys. Rev. D* 38:3657 (1988)
419. Fischbach E, Talmadge C. *Nature* 356: 207 (1992)
420. Fischbach E, Talmadge C. In *Proc. Rencontres de Moriond: Dark Matter and Cosmology, Quantum Measurements and Experimental Gravitation, 31st, Les Arcs, France, 20–27 Jan. 1996*
421. Fischbach E, Talmadge C. *The Search for Non-Newtonian Gravity*. New York: Springer (1998)
422. Franklin A. *The Rise and Fall of the Fifth Force*. New York: Am. Inst. Phys. (1993)
423. Glass EN, Szamosi G. *Phys. Rev. D* 35: 1205 (1987)
424. Glass EN, Szamosi G. *Phys. Rev. D* 39: 1054 (1989)
425. Gilliland RL, Däppen W. *Astrophys. J.* 313:429 (1987)
426. Kuhn JR. In *Advances in Helio- and Asteroseismology*, ed. J Christensen-Dalsgaard, S Frandsen. Dordrecht: Reidel (1988)
427. Ellis J, et al. *Phys. Lett.* B228:264 (1989)
428. Mohanty S, Panda PK. *Phys. Rev. D* 53:5723 (1996)
429. Lee TD, Yang CN. *Phys. Rev.* 98:1501 (1955)
430. Okun LB. *Yad. Fiz.* 10:358 (1969) [*Sov. J. Nucl. Phys.* 10:206 (1969)]
431. Blinnikov SI, Dolgov AD, Okun LB, Voloshin MB. *Nucl. Phys.* B458:52 (1996)
432. Horvat R. *Phys. Rev. D* 52:7098 (1995)
433. Horvat R. *Phys. Lett.* B366:241 (1996)
434. Will CM. *Theory and Experiment in*

Gravitational Physics. Cambridge, UK: Cambridge Univ. Press. Rev. ed. (1993)
435. Dirac PAM. *Nature* 139:323 (1937)
436. Dirac PAM. *Proc. R. Soc. London A* 165:199 (1938)
437. Williams JG, Newhall XX, Dickey JO. *Phys. Rev. D* 53:6730 (1996)
438. Shapiro II. In *General Relativity and Gravitation*, ed. N Ashby, DF Bartlett, W Wyss. Cambridge, UK: Cambridge Univ. Press (1990)
439. Morrison LV. *Nature* 241:519 (1973)
440. Damour T, Taylor JH. *Astrophys. J.* 366:501 (1991)
441. Goldman I. *Mon. Not. R. Astron. Soc.* 244:184 (1990)
442. Dearborn DS, Schramm DN. *Nature* 247:441 (1974)
443. Teller E. *Phys. Rev.* 73:801 (1948)
444. Gamow G. *Proc. Natl. Acad. Sci. USA* 57:187 (1967)
445. Pochoda P, Schwarzschild M. *Astrophys. J.* 139:587 (1964)
446. Ezer D, Cameron AGW. *Can. J. Phys.* 44:593 (1966)
447. Roeder RC, Demarque PR. *Astrophys. J.* 144:1016 (1966)
448. Shaviv G, Bahcall JN. *Astrophys. J.* 155:135 (1969)
449. Chin CW, Stothers R. *Nature* 254:206 (1975)
450. Chin CW, Stothers R. *Phys. Rev. Lett.* 36:833 (1976)
451. Demarque P, et al. *Astrophys. J.* 437:870 (1994)
452. Guenther DB, et al. *Astrophys. J.* 445:148 (1995)
453. Guenther DB, Krauss LM, Demarque P. *Astrophys. J.* 498:871 (1998)
454. Vila SC. *Astrophys. J.* 206:213 (1976)
455. García-Berro E, Hernanz M, Isern J, Mochkovitch R. *Mon. Not. R. Astron. Soc.* 277:801 (1995)
456. Benvenuto OG, Althaus LG, Torres DF. *Mon. Not. R. Astron. Soc.* In press (1999)
457. Prather MJ. *The Effect of a Brans-Dicke Cosmology upon Stellar Evolution and the Evolution of Galaxies*. PhD thesis, Yale Univ. (1976)
458. VandenBerg DA. *Mon. Not. R. Astron. Soc.* 181:695 (1977)
459. Degl'Innocenti S, et al. *Astron. Astrophys.* 312:345 (1996)
460. Thorsett SE. *Phys. Rev. Lett.* 77:1432 (1996)
461. Malaney RA, Mathews GJ. *Phys. Rep.* 229:145 (1993)
462. Gabriel MD, Haugan MP, Mann RB, Palmer JH. *Phys. Rev. Lett.* 67:2123 (1991)
463. Gabriel MD, Haugan MP, Mann RB, Palmer JH. *Phys. Rev. D* 43:308 (1991)
464. Carroll SM, Field GB. *Phys. Rev. D* 43:3789 (1991)
465. Haugan MP, Kauffmann TF. *Phys. Rev. D* 52:3168 (1995)
466. LoSecco JM, et al. *Phys. Lett.* A138:5 (1989)
467. Klein JR, Thorsett SE. *Phys. Lett.* A145: 79 (1990)
468. Krisher TP. *Phys. Rev. D* 44:R2211 (1991)
469. LoSecco JM. *Phys. Rev. D* 38:3313 (1988)
470. Gasperini M. *Phys. Rev. D* 38:2635 (1988)
471. Gasperini M. *Phys. Rev. D* 39:3606 (1989)
472. Halprin A, Leung CN. *Phys. Rev. Lett.* 67:1833 (1991)
473. Pantaleone J, Halprin A, Leung CN. *Phys. Rev. D* 47:R4199 (1993)
474. Iida K, Minakata H, Yasuda O. *Mod. Phys. Lett.* A8:1037 (1993)
475. Minakata H, Nunokawa H. *Phys. Rev. D* 51:6625 (1995)
476. Bahcall JN, Krastev PI, Leung CN. *Phys. Rev. D* 52:1770 (1995)
477. Halprin A, Leung CN, Pantaleone J. *Phys. Rev. D* 53:5365 (1996)
478. Mureika JR. *Phys. Rev. D* 56:2408 (1997)
479. Glashow SL, et al. *Phys. Rev. D* 56:2433 (1997)
480. Halprin A, Leung CN. *Phys. Lett.* B416: 361 (1998)
481. Mansour SW, Kuo TK. hep-ph/9810510 (1998)
482. Casini H, D'Olivo JC, Montemayor R,

Urrutia LF. *Phys. Rev. D* 59:062001 (1999)
483. Goldhaber AS, Nieto MM. *Rev. Mod. Phys.* 43:277 (1971)
484. Davis Jr L, Goldhaber AS, Nieto MM. *Phys. Rev. Lett.* 35:1402 (1975)
485. Fischbach E, et al. *Phys. Rev. Lett.* 73:514 (1994)
486. Lakes R. *Phys. Rev. Lett.* 80:1826 (1998)
487. Barrow JD, Burman RR. *Nature* 307:14 (1984)
488. Chibisov GV. *Sov. Phys. Usp.* 19:624 (1976)
489. Fischbach E. *Ann. Phys.* 247:213 (1996)
490. Kiers K, Tytgat MHG. *Phys. Rev. D* 57:5970 (1998)
491. Abada A, Gavela MB, Pène O. *Phys. Lett.* B387:315 (1996)
492. Abada A, Pène O, Rodríguez-Quintero J. *Phys. Rev. D* 58:073001 (1998)
493. Abada A, Pène O, Rodríguez-Quintero J. hep-ph/9810449 (1998)
494. Abada A, Pène O, Rodríguez-Quintero J. *Phys. Lett.* B423:355 (1998)
495. Arafune J, Mimura Y. *Prog. Theor. Phys.* 100:1083 (1998)